

**HEALING OF ROCK SALT AND POTASH FRACTURE  
UNDER LONG-TERM CONFINING PRESSURE**



**A Thesis Submitted in Partial Fulfillment of the Requirements for the  
Degree of Master of Engineering in Civil, Transportation and  
Geo-resources Engineering  
Suranaree University of Technology  
Academic Year 2018**

การเชื่อมประสานตัวของรอยแตกในเกลือหินและโพแทช  
ภายใต้ความดันล้อมรอบระยะยาว



นายกรกช ค่อนสะอาด

วิทยานิพนธ์นี้เป็นส่วนหนึ่งของการศึกษาตามหลักสูตรปริญญาวิศวกรรมศาสตรมหาบัณฑิต  
สาขาวิชาวิศวกรรมโยธา ขนส่ง และทรัพยากรธรณี  
มหาวิทยาลัยเทคโนโลยีสุรนารี  
ปีการศึกษา 2561

**HEALING OF ROCK SALT AND POTASH FRACTURE UNDER  
LONG-TERM CONFINING PRESSURE**

Suranaree University of Technology has approved this thesis submitted in partial fulfillment of the requirements for a Master's Degree.

Thesis Examining Committee



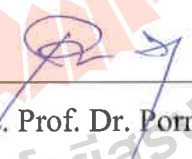
(Asst. Prof. Dr. Akkhapun Wannakomol)

Chairperson



(Asst. Prof. Dr. Decho Phueakphum)

Member (Thesis Advisor)



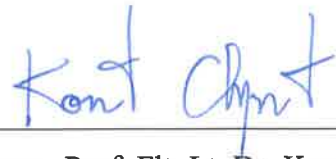
(Assoc. Prof. Dr. Pornkasem Jongpradist)

Member



(Prof. Dr. Santi Maensiri)

Vice Rector for Academic Affairs  
and Internationalization



(Assoc. Prof. Flt. Lt. Dr. Kontorn Chamniprasart)

Dean of Institute of Engineering

กรกช ก่อนสะอาด : การเชื่อมประสานตัวของรอยแตกในเกลือหินและโพแทช ภายใต้  
ความดันล้อมรอบระยะยาว (HEALING OF ROCK SALT AND POTASH FRACTURE  
UNDER LONG-TERM CONFINING PRESSURE) อาจารย์ที่ปรึกษา :  
ผู้ช่วยศาสตราจารย์ ดร. เดโซ เพื่อภุมิ, 64 หน้า

ประสิทธิภาพการเชื่อมประสานตัวของรอยแตกในตัวอย่างเกลือหินและโพแทช ได้ถูก  
ทดสอบภายใต้ความเค้นล้อมรอบคงที่ (3-20 เมกะปาสกาล) โดยการตรวจวัดการเปลี่ยนแปลงค่า  
ความชื้นผ่านของรอยแตกภายใต้ความเค้นคงที่เป็นเวลา 21 วัน การให้แรงแบบเส้นบนรอยแตกที่มี  
การประสานตัวใช้เพื่อทำการประเมินประสิทธิภาพการเชื่อมประสานตัว ผลการทดสอบระบุว่า  
ความเค้นกดล้อมรอบและเวลาสามารถลดค่าความชื้นผ่านของรอยแตกและสามารถเพิ่ม  
ประสิทธิภาพการประสานตัว กระบวนการเชื่อมประสานตัวของรอยแตกเกี่ยวข้องกับแรงโควาเลนต์  
และการตกผลึกใหม่ ทั้งสองกระบวนการสามารถปรับปรุงประสิทธิภาพของคุณสมบัติทางกลศาสตร์  
และพลศาสตร์ ความชื้นผ่านและการเชื่อมประสานตัวของรอยแตกเกลือหินและโพแทช ถูกนำมา  
สร้างความสัมพันธ์กับพลังงานความเครียดเฉลี่ยที่ได้รับ ผลดังกล่าวสามารถนำมาคาดคะเน  
พฤติกรรมการประสานตัวภายใต้สภาวะจริง (ความเค้นล้อมรอบ) ความลึกของช่องเปิดและ  
ระยะเวลาในการปิดผนึกเป็นปัจจัยหลักที่ควบคุมคุณภาพทางพลศาสตร์และ เชิงกลศาสตร์ที่  
ระยะเวลานาน ซึ่งสามารถสรุปได้ว่าค่าความชื้นผ่านของรอยแตกที่อยู่ระดับลึกมีค่าลดลงอย่าง  
รวดเร็วเมื่อเทียบกับรอยแตกระดับตื้น ภายใต้พลังงานความเครียดเฉลี่ยที่เท่ากัน รอยแตกของเกลือ  
หินสามารถประสานตัวได้ดีกว่ารอยแตกในโพแทช ระยะเวลาของการเชื่อมประสานตัวเป็นอีก  
หนึ่งปัจจัยหลักที่ควบคุมการเชื่อมประสานตัวของรอยแตกในเกลือหินและโพแทช

สาขาวิชา เทคโนโลยีธรณี  
ปีการศึกษา 2561

ลายมือชื่อนักศึกษา กรกช  
ลายมือชื่ออาจารย์ที่ปรึกษา เดโซ

KORAKOT KONGSAARD: HEALING OF ROCK SALT AND POTASH  
FRACTURE UNDER LONG-TERM CONFINING PRESSURE. THESIS  
ADVISOR: ASST. PROF. DECHO PHUEKPHUM, Ph.D., 64 PP.

PERMEABILITY/ HYDROSTATIC STRESS/ MEAN STRAIN ENERGY

Long-term healing test under constant hydrostatic stresses (3-20 MPa) has been performed to assess the healing effectiveness of fractures in rock salt and potash specimens. Gas flow testing has been conducted to monitor the changes of fracture permeability under constant stresses for up to 21 days. Line-loading on the healed fractures has been performed to assess the healing effectiveness. The results show that hydrostatic stresses and durations can decrease fracture permeability and increase healing effectiveness. Healing mechanism of fractures involves covalent bonding and recrystallization. These can improve the mechanical and hydraulic performance. The permeability and healing effectiveness of salt and potash fractures have been derived as a function of the applied mean strain energy, primarily to allow predicting their healing behavior under in-situ conditions. The opening depth and duration at which sealing is taken place are significant factors controlling its long-term hydraulic and mechanical performance. The findings imply that permeability of fractures at greater depths may be reduced quicker than those at shallower depths. Under the same mean strain energy, salt fractures can be healed better than potash fractures. Healing duration is one of the main factor that controlling the healing of salt and potash fractures.

School of Geotechnology

Academic Year 2018

Student's Signature กษณกร

Advisor's Signature เดโช

## ACKNOWLEDGMENTS

I wish to acknowledge the funding support from Suranaree University of Technology (SUT).

I would like to express my sincere thanks to Prof. Dr. Kittitep Fuenkajorn for his valuable guidance and efficient supervision. I appreciate his strong support, encouragement, suggestions and comments during the research period. I also would like to express my gratitude to Asst. Prof. Dr. Decho Phueakphum and Asst. Prof. Dr. Prachya Tepnarong for their constructive advice, valuable suggestions and comments on my research works as thesis committee members. Grateful thanks are given to all staffs of Geomechanics Research Unit, Institute of Engineering who supported my work.

Finally, I would like to thank beloved parents for their love, support and encouragement.

มหาวิทยาลัยเทคโนโลยีสุรนารี

Korakot Konsaard

# TABLE OF CONTENTS

	<b>Page</b>
ABSTRACT (THAI) .....	I
ABSTRACT (ENGLISH).....	II
ACKNOWLEDGEMENTS.....	III
TABLE OF CONTENTS.....	IV
LIST OF TABLES.....	VII
LIST OF FIGURES .....	VIII
SYMBOLS AND ABBREVIATIONS.....	XI
<b>CHAPTER</b>	
<b>I INTRODUCTION.....</b>	<b>1</b>
1.1 Background and rationale .....	1
1.2 Research objectives.....	2
1.3 Research methodology.....	2
1.3.1 Literature review.....	4
1.3.2 Sample preparation.....	4
1.3.3 Laboratory testing.....	4
1.3.4 Hydraulic and Mechanical parameters .....	5

## TABLE OF CONTENTS (Continued)

	<b>Page</b>
1.3.5 Applications .....	5
1.3.6 Discussions, conclusions and thesis writing.....	5
1.4 Scope and limitations .....	6
1.5 Thesis contents .....	6
<b>II LITERATURE REVIEW .....</b>	<b>8</b>
2.1 Introduction.....	8
2.2 Healing effectiveness .....	8
2.3 Permeability .....	17
<b>III SAMPLE PREPARATION .....</b>	<b>22</b>
3.1 Introduction.....	22
3.2 Sample preparation .....	22
<b>IV LABORATORY TESTING METHODS AND RESULTS .....</b>	<b>26</b>
4.1 Introduction.....	26
4.2 Test methods .....	26
4.3 Test results .....	29
4.3.1 Hydraulic Properties .....	29
4.3.2 Healing Effectiveness .....	31
4.3.3 Strain Energy Principle.....	35
<b>V DERIVATION OF EMPIRICAL EQUATIONS .....</b>	<b>39</b>
5.1 Introduction.....	39



## TABLE OF CONTENTS (Continued)

	<b>Page</b>
5.2 Hydraulic properties.....	39
5.2.1 Hydraulic aperture .....	39
5.2.2 Intrinsic permeability.....	40
5.3 Healing effectiveness .....	42
5.4 Mean strain energy.....	45
<b>VI DAMAGE RECOVERY .....</b>	<b>51</b>
6.1 Introduction.....	51
6.2 Borehole in salt and potash mass subjected to uniform external pressure .....	51
6.3 Prediction of salt and potash after sealing .....	54
<b>VII DISCUSSIONS AND CONCLUSIONS .....</b>	<b>60</b>
7.1 Discussions .....	60
7.2 Conclusions.....	62
7.3 Recommendations for future studies .....	64
REFERENCES .....	65
BIOGRAPHY .....	72

## LIST OF TABLES

Table	Page
3.1 Dimension of salt and potash specimens.....	25
4.1 Line load test results of salt and potash specimens with tension-induced fractures and saw-cut surfaces after healing under confining pressures.....	35
5.1 Empirical constants obtained for hydraulic aperture of salt and potash fracture as a function time under various pressures.....	40
5.2 Empirical constants obtained for intrinsic permeability of salt and potash fractures under various pressures.....	42
5.3 Empirical constants obtained for healing effectiveness of salt and potash fracture as a function pressure.....	44
5.4 Empirical constants obtained for healing effectiveness of salt and potash fractures under various pressure as a function time.....	45
5.5 Empirical constants obtained for hydraulic aperture of salt and potash fractures as a function means strain energy.....	47
5.6 Empirical constants obtained for intrinsic permeability of salt and potash fractures as a function means strain energy.....	48
5.7 Empirical constants obtained for healing effectiveness of salt and potash fractures as a function means strain energy.....	49

## LIST OF FIGURES (Continued)

Figure	Page
5.2	Intrinsic permeability of salt (a) and potash (b) as a function time.....43
5.3	Healing effectiveness of salt and potash as a function pressure.....44
5.4	Healing effectiveness with Fuenkajorn and Phueakphum (2011) as a function comparison times. ....46
5.5	Hydraulic aperture of salt and potash as a function mean strain energy.....47
5.6	Intrinsic permeability of salt and potash as a function mean strain energy. ....48
5.7	Healing effectiveness of salt and potash as a function mean strain energy. ....50
6.1	Release mean strain energy of borehole closure in salt and potash as a function times. ....54
6.2	Remaining mean strain energy ( $\Delta W_m$ ) as a function of time after sealing.....56
6.3	Hydraulic aperture ( $e_h$ ) of salt and potash as a function time after sealing.....57
6.4	Intrinsic permeability ( $k_i$ ) of salt and potash as a function time after sealing..58
6.5	Healing effectiveness ( $H_e$ ) of salt and potash as a function time after sealing.....59

## LIST OF FIGURES

Figure	Page
1.1 Research Methodology.....	3
2.1 Healing test under uniaxial loading. The specimens are loaded axially by means of a dead weight consolidation machine .....	10
2.2 Specimens with tension-induced fracture (a) and with polished.....	10
2.3 Hydraulic conductivity ( $K_f$ ) of five tension-induced fractures as a function of time (t) under radial loading .....	11
2.4 Healing effectiveness as a function of healing time under axial loading on the tension-induced fractures at ambient temperature.....	16
2.5 Healing effectiveness as a function of healing time under hydrostatic stresses loading at ambient temperature and at elevated temperature of 200°C .....	16
2.6 P-wave velocities ( $H_e$ ) as a function of time (t) of tension-induced fractures at uniaxial stresses 0.5 MPa. P-wave velocities ( $H_e$ ) as a function of time (t) of tension-induced fractures at ambient temperature.....	18
3.1 Salt (a) and potash (b) specimens.....	23
3.2 Line load to induce tensile fracture .....	24
3.3 Saw-cut device .....	24
3.4 Specimens with tensile fracture (a) and saw-cut surface (b).....	24
4.1 True triaxial load device (a) and test specimen with drilled hole connected to nitrogen gas tank via high-pressure tube (b).....	28

## LIST OF FIGURES (Continued)

Figure	Page
4.2	Line load device and area of the radial flow path. ....28
4.3	Outflow rates (Q) of tension-induced fractures in salt (a) and potash as a function time under various confining pressures (P). ....30
4.4	Outflow rates (Q) of saw-cut fracture in salt as a function time under confining pressures (P). ....31
4.5	Hydraulic apertures ( $e_h$ ) of tension induced fractures in salt (a) and potash (b) as a function times (t). ....32
4.6	Intrinsic permeability ( $k_i$ ) of specimens with tension-induced fractures in salt (a) and potash (b) as a function time under various confining pressures (P)...33
4.7	Intrinsic permeability ( $k_i$ ) of specimens with saw-cut surface in salt as a function time under confining pressures (P) .....34
4.8	Fractures healing after test of tension induced fracture in salt (a) and potash (b). ....34
4.9	Healing effectiveness ( $H_e$ ) of tension induced fracture in salt and potash as function time under various confining pressures. ....36
4.10	Hydraulic aperture in salt and potash as a function mean strain energy.....37
4.11	Intrinsic permeability of salt and potash as a function mean strain energy. ....37
4.12	Healing effectiveness in salt and potash as a function mean strain energy. ....38
5.1	Hydraulic aperture of salt (a) and potash (b) as a function of time under various pressures. ....41

## SYMBOLS AND ABBREVIATIONS

$\alpha$	=	Empirical constant for equation 5.2
$\alpha'$	=	Empirical constant for equation 5.10
$\beta$	=	Empirical constant for equation 5.2
$\beta'$	=	Empirical constant for equation 5.10
$\gamma$	=	Empirical constant for equation 5.3
$\gamma'$	=	Empirical constant for equation 5.11
$\gamma_g$	=	Unit weight of nitrogen gas
$\gamma_b$	=	Material constants of the potential creep law for equation 6.8
$\delta$	=	Empirical constant for equation 5.3
$\delta'$	=	Empirical constant for equation 5.11
$\epsilon_\theta$	=	Tangential strain
$\epsilon_m$	=	Mean strain of fractures closure
$\epsilon_r$	=	Radial strain
$\epsilon_z$	=	Axial strain
$\epsilon_r^e$	=	Elastic radial strain
$\epsilon_r^c$	=	Time-dependent radial strain controlling the creep closure of the borehole
$\zeta$	=	Empirical constant for equation 5.5
$\eta$	=	Empirical constant for equation 5.5

## SYMBOLS AND ABBREVIATIONS (Continued)

$\phi$	=	Diameter
$\iota$	=	Empirical constant for equation 5.6
$\kappa$	=	Empirical constant for equation 5.6
$\kappa_b$	=	Material constants of the potential creep law for equation 6.8
$\lambda$	=	Empirical constant for equation 5.7
$\mu_g$	=	Dynamic viscosity of nitrogen gas
$\nu$	=	The Poisson's ratio
$\upsilon$	=	Empirical constant for equation 5.7
$\xi$	=	Empirical constant for equation 5.8
$\rho$	=	Density of the specimen
$\rho_c$	=	Density of carnallite (1.60 g/cc)
$\rho_s$	=	Density of halite (2.16 g/cc)
$\zeta$	=	Empirical constant for equation 5.8
$\sigma_1$	=	Axial stress
$\sigma_2$	=	Lateral stresses
$\sigma_3$	=	Lateral stresses
$\sigma_r$	=	Radial stress
$\sigma_\theta$	=	Tangential stress
$\sigma_m$	=	Mean stresses
$\sigma_z$	=	Axial stresses

## SYMBOLS AND ABBREVIATIONS (Continued)

$\sigma^*$	=	Equivalent (effective) stress
$\tau$	=	Empirical constant for equation 5.8
$\phi$	=	Empirical constant for equation 5.8
$\chi$	=	Empirical constant for equation 5.9
$\omega$	=	Empirical constant for equation 5.9
$a$	=	Borehole radius
$C\%$	=	Carnallite content
$E$	=	Elastic modulus
$e_h$	=	Hydraulic aperture
$F_h$	=	Fracture tensile strength
$F_i$	=	Intact tensile strength
$H_e$	=	Healing effectiveness
$k_i$	=	Intrinsic permeability
$P$	=	Pressures
$P_o$	=	External pressures
$\Delta P$	=	Difference pressures injection and ambient pressures (psi)
$Q$	=	Flow rate
$r$	=	Radial distance from the center
$r_{in}$	=	Radius of the injection hole
$r_{out}$	=	Radial of outflow boundary



## SYMBOLS AND ABBREVIATIONS (Continued)

$S_r$	=	Radial stress deviation
$t$	=	Time
$t_0$	=	Time at which loading is applied (usually assumed to be zero)
$t_1$	=	Time at which the strains are calculated
$\Delta t$	=	Duration of healing
$t_i$	=	Period as if no borehole sealing
$t_s$	=	Time at which sealing
$W_{m,s}$	=	Mean strain energy of salt
$W_{m,PT}$	=	Mean strain energy of potash
$W_{m,r}$	=	Total released energy from drilling
$W_{m,l}$	=	Energy lost due to creep closure before sealing
$\Delta W_m$	=	Remaining mean strain energy

# CHAPTER I

## INTRODUCTION

### 1.1 Background and rationale

The challenges on the underground excavation in salt and potash for underground facilities (e.g. compressed-air energy storage, natural gas storage, nuclear waste disposal in salt mining) are that the cracks or fractures induced by naturally occurring and the damage during excavation may cause instability of the surrounding salt and potash leakage of storage materials from cavern. Self-healing can impel the fracture of damaged salt and potash, thereby improving the mechanical properties and permeability of damaged salt and potash inside the cavern. Damage in salt and potash which generally manifests in the form of micro-cracks and fractures can be recovered or healed when subjected to sufficiently stresses. When cracks are closed, permeability can be reduced by several orders of magnitude (Renard, 1999). The presence of damage in the form of micro-cracks in salt and potash can alter the structural stability and permeability of salt affecting the integrity of a repository (Chen et al., 1997). The healing of salt and potash fractures around opening also affects the mechanical stability of the opening (Katz and Lady, 1976). The size reduction of the micro-cracks can increase the salt and potash stiffness and strength. The main driving force for fracture healing is a minimization of surface tension, and creation of contact areas and covalent bonds between the two surfaces of the fractures. The fractures are formed by separation or splitting of salt crystals, it can

easily healed even under relatively low stress for a short period, But the fracture surface is coated with any inclusions, healing will not occur (Fuenkajorn and Phueakphum, 2011).

## **1.2 Research objectives**

The objective of this study is to assess the healing effectiveness of salt and potash fractures as a function of pressures conditions, fracture types and durations. The healing tests can be performed under confining pressures varying from 3 to 20 MPa for salt and 5 to 15 MPa for potash up to 21 days. The nitrogen gas flow testing is performed to determine the out-flow rate and intrinsic permeability of fractures that changes over time. The out-flow rates under constant head are continuously monitored every 12 hours for 21 days of each test conditions using a flow meter (10 cc/min). The line load test of each the specimen measured before and after healing are compared to assess the healing effectiveness of the fracture. The mathematical relationships between the permeability and healing effectiveness are developed as a function pressures, duration and mean strain energy.

## **1.3 Research methodology**

The research methodology as shown in Figure 1.1 comprises 7 steps; including literature review, sample preparation, laboratory testing, derivation of empirical equations, application, discussions and conclusions, and thesis writing.

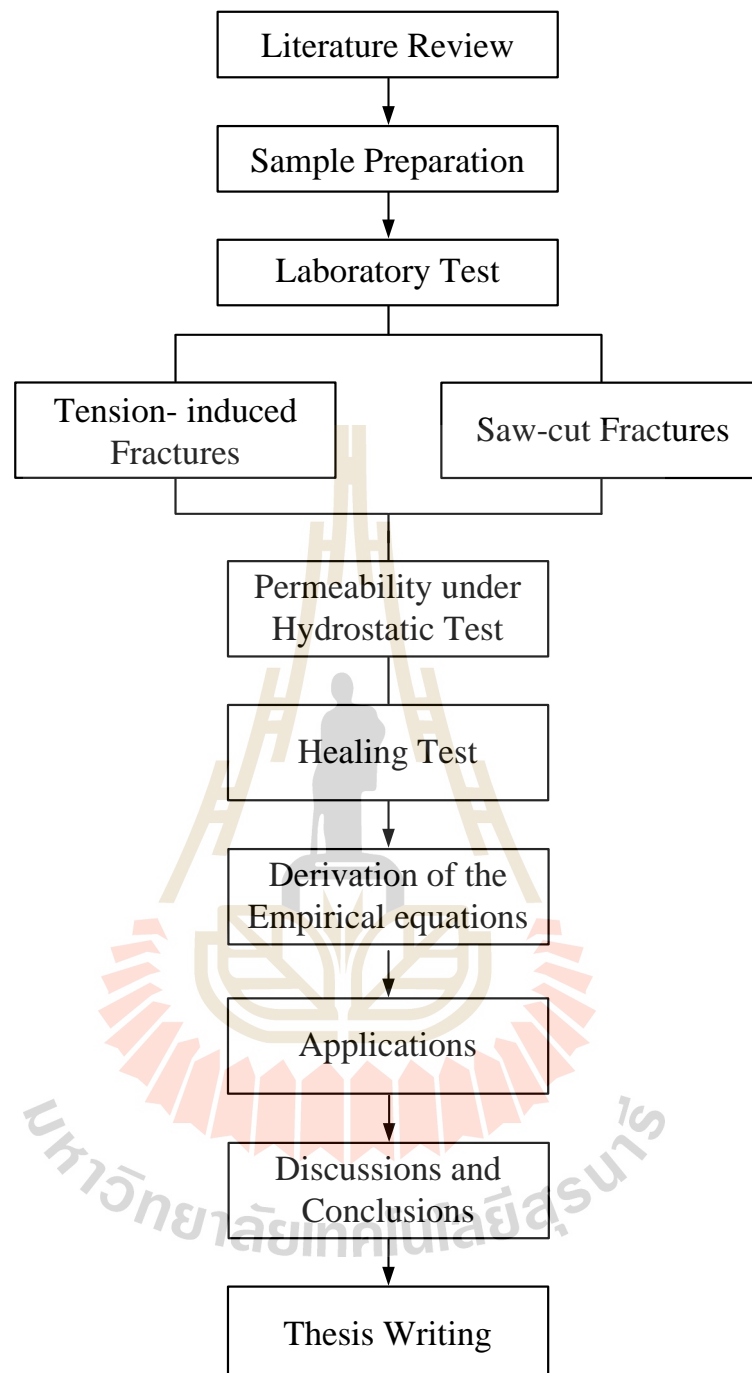


**Figure 1.1** Research methodology.

### **1.3.1 Literature review**

Literature reviews are carried out to study the previous researches on the mechanical and hydraulic mechanism of healing fractures under confining pressures and duration. The mechanism of fracture healing and the method to measure the healing effectiveness by using line load test and permeability of fracture test are summarized. The sources of information are from text books, journals, technical reports and conference papers. A summary of the literature review is given in the thesis.

### **1.3.2 Sample preparation**

The salt and potash specimens used here are obtained from the Middle and Lower member of the Maha Sarakham Formation, northeastern Thailand. Warren (1999) and Suwanich (1986) give detailed descriptions of the salt and geology of the basin. The specimens are from depth ranging between 250 m and 400 m. The drilling is carried out by the ASEAN Potash Mining Co., Ltd. The tensile strengths of salt and potash are determined for designing the healing test parameters. The nominal dimensions of block specimens are  $50 \times 50 \times 100 \text{ mm}^3$ . The sample preparation and test procedures follow as much as practical the ASTM standard practices (i.e., ASTM D3967-95).

### **1.3.3 Laboratory testing**

The healing tests on the tension-induced fractures are under hydrostatic stresses range from 3 to 20 MPa for salt and 5 to 15 MPa for potash. Saw-cut fractures are subjected to the stresses between 10 and 20 MPa. The true triaxial loading device is used to apply the constant axial and lateral pressures to the specimens. The nitrogen gas flow testing is performed to determine the permeability

of fractures that changes over duration. The out-flow rates under constant head are continuously monitored every 12 hours for 21 days of each test conditions using a flow meter (10 cc/min). Nitrogen gas is injected under 69 kPa (10 psi) into the tube to measure the fracture flow rate.

#### **1.3.4 Hydraulic and Mechanical parameters**

Regression analysis on the test data by SPSS software (Colin and Paul, 2012) can determine parameters for the hydraulic aperture, intrinsic permeability and healing effectiveness. The functions can be used to prediction the healing of fractures under pressures conditions beyond the test parameters.

Results from laboratory measurements in terms of pressures and duration of salt and potash are used to develop hydraulic aperture, intrinsic permeability and healing effectiveness criteria relationship between pressure, duration and mean strain energy.

#### **1.3.5 Applications**

The proposed equations are used to predict the mechanical (healing effectiveness) and hydraulic performance (hydraulic aperture and intrinsic permeability) of fractures around the salt and potash opening, such as the exploration borehole.

#### **1.3.6 Discussions, conclusions and thesis writing**

Discussions are made on the reliability and adequacies of the approaches used here. Future research needs are identified. All research activities, methods, and results are documented and compiled in the thesis. The research or findings are published in the conference proceedings or journals.

## 1.4 Scope and limitations

The scope and limitations of the research include as follows.

- 1) All tests are conducted on the salt and potash specimens obtained from the Maha Sarakham formation.
- 2) Two types of fractures are prepared for testing; tension-induced fractures and saw-cut fractures formed by saw-cut. All fractures should be well mated.
- 3) The test procedures will follow the relevant ASTM standard practices, as much as practical.
- 4) All tests are performed under dry condition up to 21 days.
- 5) The tension-induced fractures are subjected to constant hydrostatic stresses at 3, 5, 7, 10, 15 and 20 MPa for salt, and 5, 7, 10 and 15 for potash. saw-cut fractures applied constant hydrostatic stress at 10 and 20 MPa only salt.
- 6) The temperatures are ambient.
- 7) Gas flow permeability tests are performed every 12 hours for 21 days to assess the healing effectiveness.
- 8) The mechanical testing; the line load tests on healed fracture are performed to assess the mechanical performance of the fractures after healing.

## 1.5 Thesis contents

Chapter I describes the objectives, the problems and rationale, and the methodology of the research. Chapter II present results of the literature review on healing effectiveness of salt and potash fractures under stresses and permeability of

salt and potash fractures. Chapter III describes the salt sample collection and preparation. Chapter IV describes the laboratory testing and test results. Chapter V derive the empirical equations. Chapter VI predict the damage recovery after sealing in borehole. Chapter VII provides the discussion, conclusion and recommendations for future research studies.





# CHAPTER II

## LITERATURE REVIEW

### 2.1 Introduction

Literature reviews are carried out to study the previous researches on the mechanical and hydraulic mechanism of healing fractures under confining pressures and duration. The mechanism of fracture healing and the method to measure the healing effectiveness by using line load test and permeability of fracture test are summarized. The sources of information are from text books, journals, technical reports and conference papers. The initial literature reviews are summarized as follows.

### 2.2 Healing effectiveness

Damage or fractures in rock salt formations can be healed under hydrostatic and non-hydrostatic compression. When cracks are closed, permeability can be reduced by several orders of magnitude (Renard, 1999). The healing capability of fractures is one of the advantages for rock salt to be used as a host rock for nuclear waste repository in the United States and Germany (Habib and Berest, 1993). The presence of damage in the form of micro-cracks in salt can alter the structural stability and permeability of salt, affecting the integrity of a repository (Chan et al., 1998a). The healing of rock salt fractures around air or gas storage caverns also affects the designed storage capacity and the mechanical stability of the caverns (Katz and Lady,

1976) Miao et al. (1995) state that the healing of rock salt is probably due to the visco-plastic deformation of grains, causing the closure of cracks and pore spaces. The size reduction of the micro-cracks can increase the salt stiffness and strength. The main driving force for fracture healing is a minimization of surface tension, and creation of contact areas and covalent bonds between the two surfaces of the fracture. It is defined here that healing is the closure of fractures without any precipitation of materials inside. It is a chemical and physical process in which the material properties evolve with time or in which the defects (voids and cracks) decrease. The initiation, propagation and healing of fractures in salt mass around underground structures have long been recognized; most investigations however have concentrated on their impact on the mechanical constitutive behavior of the rock (e.g., Allemandou and Dusseault, 1993; Munson et al., 1999; Costin and Wawersik, 1980). Several experimental researches on the healing and consolidation of crushed salt in wet conditions and conclude have also been carried out in an attempt at understanding the healing behavior between the salt particles and their impact on the bulk properties (e.g., Ouyang and Daemen, 1989; Miao et al., 1995). After the healing takes place, density, inelastic strain, Young's modulus and strength of the crushed salt increase as the time increases. A direct experimental assessment of the healing behavior of individual salt fractures remains rare.

Fuenkajorn and Phueakphum (2011) performed the laboratory testing to assess the healing effectiveness of rock salt fractures as affected by the stress conditions, fracture types, and time. The effort involved healing tests under uniaxial and radial loading (Figures 2.1 and 2.2), gas flow permeability tests to monitor the time-dependent behavior of the salt fractures, and point loading and diameter loading tests

to assess the mechanical performance of the fractures after healing. Healing tests under static loading are carried out under both dry and saturated conditions.

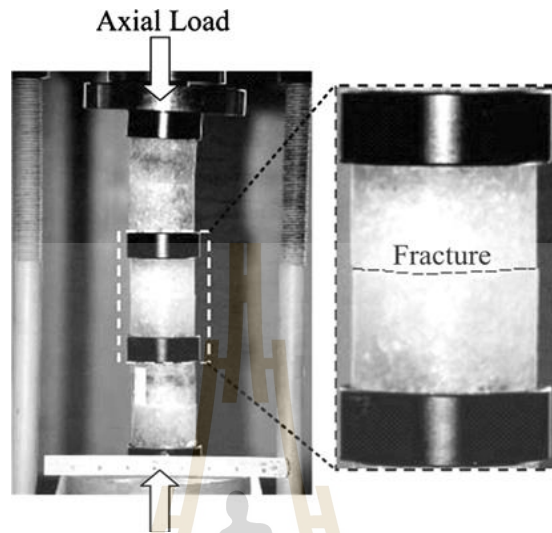


**Figure 2.1** Healing test under uniaxial loading. (Fuenkajorn and Phueakphum, 2011).

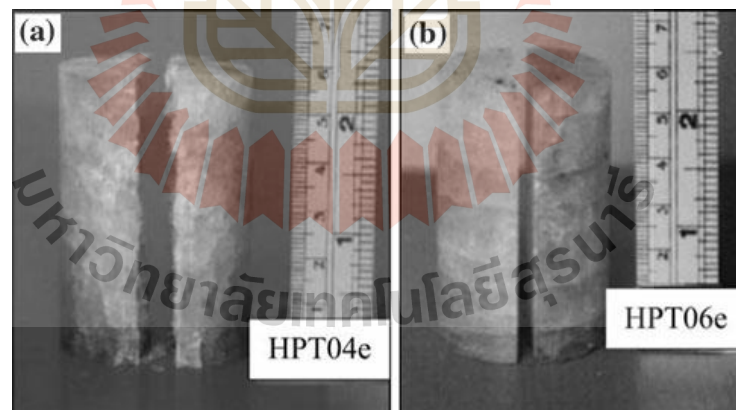


**Figure 2.2** Specimens with tension-induced fracture (a) and with polished fracture (b) (Fuenkajorn and Phueakphum, 2011).

The results suggest that the primary factors governing the healing of salt fractures are the origin and purity of the fractures, the magnitude and duration of the

fracture pressurization. Inclusions or impurities significantly reduce the healing effectiveness. The hydraulic conductivity of the fractures in pure salt can be reduced permanently by more than 4 orders of magnitude under the applied stress of 20 MPa for a relatively short period, as shown in Figure 2.3. For most cases the reduction of salt fracture permeability is due to the fracture closure which does not always lead to fracture healing. The closure involves visco-plastic deformation of the asperities on both sides of the salt fracture, while the healing is related to the covalent bonding between the two surfaces. Fracture roughness and brine saturation apparently have an insignificant impact on the healing process.

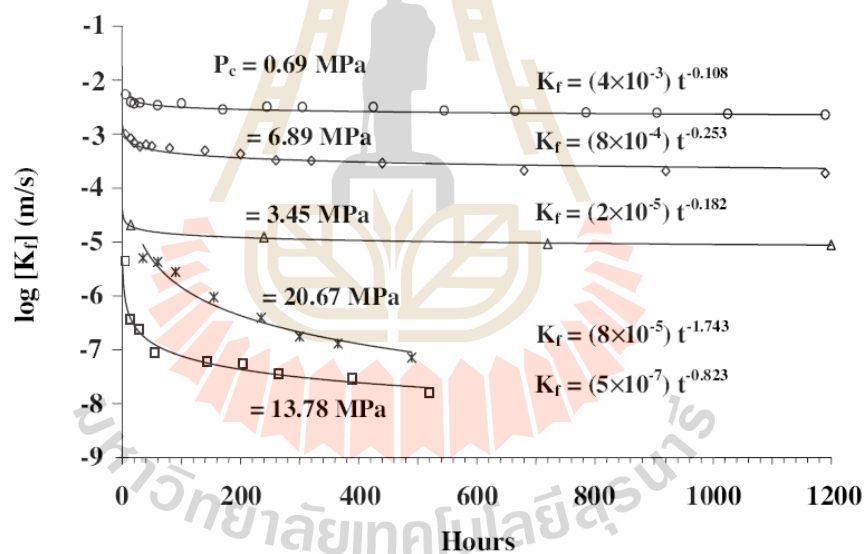


**Figure 2.3** Hydraulic conductivity ( $K_f$ ) of tension-induced fractures as a function of time ( $t$ ) under radial loading (Fuenkajorn and Phueakphum, 2011).

Healing is closure of fractures or faults without any precipitation of matters inside the fracture. It is a chemical and physical process in which the material

properties evolve with time or in which defects including voids and cracks decrease. Healing of rock salt due to visco-plastic deformation of grain, causing the closure of crack and pore space. There are two healing mechanisms, closure of micro-cracks and healing of micro-crack. It implies that micro-cracks and micro-voids reduce in size, with a corresponding increase in stiffness and strength (Miao et al., 1995). The main driving force for crack healing is a minimization of surface tension. Healing occurs by creation of contact areas and covalent bonds between the two surfaces of the fracture. It involves a local transport of mineral material. The most important factors that may affect the rate of crack healing are time, stress, temperature, saturation, contact area and geometry of contact surface, and chemical effects that may alter diffusion coefficient (Renard, 1999). In most cases, crack healing is achieved grain size scale (micrometer to millimeter). The only way to observe healed crack may be through some tiny fluid inclusions which can be related to deformation phases or metamorphic conditions.

Healing of rock fractures has occurred on various scales. In geology, fracture healing is an important mechanism controlling the circulation of fluid in the earth crust (Renard, 1999). In a smaller scale, circulation of solution or fluid in rock mass can result in a precipitation or deposition of minerals and ores in fracture zone. When fractures are open, fluid can percolate and react with in the rock (dissolution, precipitation of minerals, ore, etc.). This process notably modifies the fluid circulation and interactions between the lower crust and the surface. Healing reduces the fluid flow between fault zones. Healing of fractures or faults induced in rock salt formations can prevent the brine flow from contaminating the upper surface or nearby rock formations. The presence of damage in the form of micro cracks in salt can alter

the structural stability and permeability of salt, affecting the integrity of a repository (Chan et al., 1998b). When cracks are closed, permeability can be reduced by several orders of magnitude. The healing capability of fractures is one of the advantages for rock salt to be used as a host rock for nuclear waste repository in the United States and Germany (Habib and Berest, 1993; Broek and Heilbron, 1998). The healing process of rock salt fractures around an air or gas storage cavern also affects the designed storage capacity and the mechanical stability of the cavern (Katz and Lady, 1976). Numerous studies of fracture healing given in the literature review by Miao et al. (1995) include, for example, the crack healing in geological, the curing concrete, the recovery and recrystallization of metals, and the liquid-phase-enhanced densification of granularly crystalline materials. In rock salt the study on crushed rock salt samples with small amounts water is capable of healing during densification creep processes (Miao et al., 1995). A treatment of damage healing in crushed salt was presented by Miao et al. (1995). In this formulation, a healing surface in the sense of a yield surface in classical plasticity theory is used in conjunction with loading and unloading conditions.

Chan et al. (1994; 1995) and Munson et al. (1999) proposed a constitutive formulation for treating damage healing in damaged intact salt, referred to as the multi-mechanism deformation coupled fracture (MDCF) model, which is based on a generalized damage evolution equation that includes both a damage generation term and a healing term. Because, both damage generation and healing are treated, the MDCF model is suitable for treating damage accumulation and healing in disturbed rock zone in the repository at Waste Isolation Pilot Plant (WIPP) site (Chan et al., 2000).

Fracture healing of material, mechanics closer and connect of fracture. By this procedure except fracture healing by the sediment of substance in the fracture, fracture healing occurs on many factors, for example times, stress, temperature, humidity and characteristic of fracture (Renard, 1999). Two healing mechanisms are (1) fracture closer on compression for connect fracture and (2) fracture healing by chemical and physical procedure, material necessary of time-dependence for fracture healing (Chan et al., 1995, 1996a, 1996b 1997, 2000; Miao et al., 1995; Munson et al., 1999). Fracture healing can be investigated by electron microscope for detection of fracture healing.

Brodsky and Munson (1994) studied the healing in rock salt fractures which is a part of project named “Waste Isolation Pilot Plant” (WIPP). The cylindrical shaped rock salt specimen was stored in a Hock cell under hydrostatic pressure of 0.5 MPa and at temperature of 25°C. The specimen is then compressed in the axial direction to cause a little displacement. After that, the temperature is varied to be 20°C, 46°C and 70°C for each specimen to study the effect from temperature changes. The specimen is loaded with a strain rate of  $1 \times 10^{-6} \text{ sec}^{-1}$ . Ultrasonic wave velocity test has been also employed to use in conjunction with the test. The derived data have been using as a basic information for comparison with the result from MDCF model created to evaluate healing in anisotropic fracture of rock salt. The results have significant implications for sealing systems because they demonstrate that the healing process is quite rapid compared to the creep closure process.

Allemandou and Dusseault (1993) studied the healing of fracture by applying triaxial compressive stress at confining pressure of 2 MPa and constant axial load. The cylindrical shaped rock salt specimen is subjected to the above-mentioned stress



under constant temperature within several hours. After that the axial stress is changed to be 10, 15, 20, and 25 MPa, respectively. Assessment of closing and healing of fracture from the CAT-scan reveals that healing takes place and voids decrease as stress level increases.

Munson et al. (1999) developed a constitutive model for representing inelastic flow due to coupled creep, damage, and healing in rock salt is presented in this paper. This constitutive model, referred to as Multimechanism Deformation Coupled Fracture (MDCF) model, has been formulated by considering individual mechanisms that include dislocation creep, shear damage, tensile damage, and damage healing. Applications of the model to representing the inelastic flow and fracture behavior of WIPP salt subjected to creep, quasi-static loading, and damage healing conditions are illustrated with comparisons of model calculations against experimental creep curves, stress-strain curves, strain recovery curves, time-to-rupture data, and fracture mechanism maps.

Charoenpiew (2015) assesses the healing effectiveness of rock salt fractures as affected by the stress conditions, fracture types, time and temperatures. The effort involved healing tests varied constant axial stresses and hydrostatic stresses within 56 days. The temperatures are varied for healing under uniaxial stresses Figure 2.4 shows the healing effectiveness as a function of healing time under axial at ambient temperature and Figure 2.5 shows the healing effectiveness as a function of healing time under hydrostatic stresses loading at elevated temperature of 200°C.



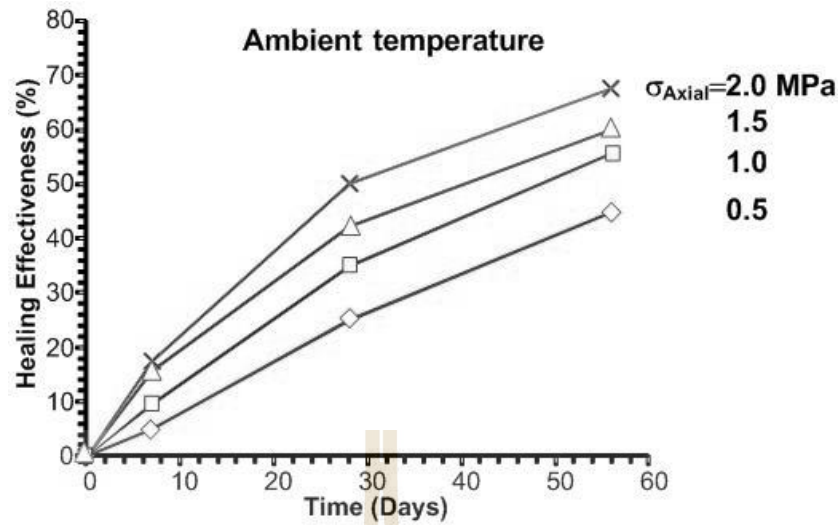


**Figure 2.4** Healing effectiveness as a function of healing time under axial loading at ambient temperature (Charoenpiew, 2015).

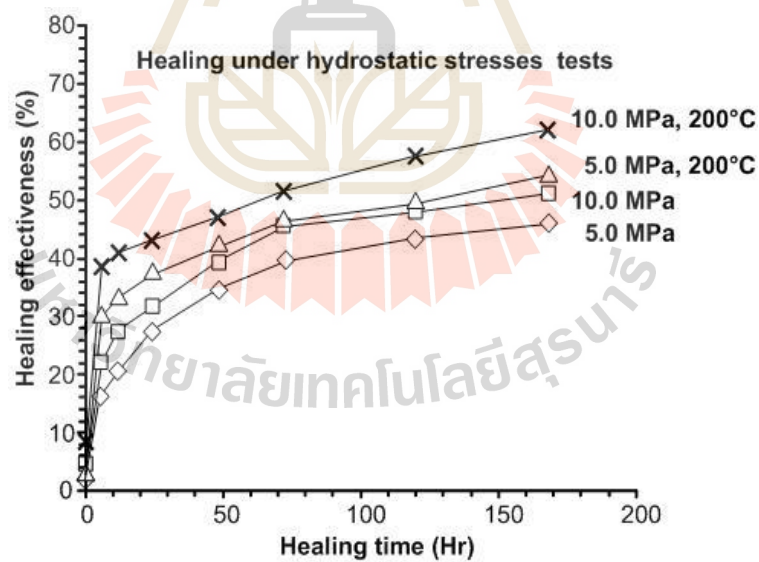


**Figure 2.5** Healing effectiveness as a function of healing time under hydrostatic stresses loading at ambient temperature and at elevated temperature of 200°C (Charoenpiew, 2015).

The ultra-sonic wave, P-wave and S-wave are monitored on healed fractures under axial stresses for every 7 days throughout 56 days. The point load tests with the healed fractures under axial stresses and line load tests with healed fracture under hydrostatic stresses are performed to assess the mechanical performance of the fractures after healing. The results indicated that Series I, the saw-cut fractures remained separable with no healing, Series II, Series III: The healing effectiveness increase with increasing stresses and time these agree with the experimental results on rock salt performed by (Fuenkajorn and Phueakphum, 2011). The wave velocity of the rock salt Figure 2.6 shown increases rapidly during the first 7 days, and after that the P-wave are slightly increases steadily with time. For healing under hydrostatic stresses tests, the results indicate that healing effectiveness tended to increase with increasing healing time and hydrostatic stresses. The recovery of ultrasonic wave characteristics depended upon both pressure and damage level (Brodsky, 1990). Temperatures slightly increase the healing effectiveness.

## 2.2 Permeability

Stormont and Daemen (1991) studied the permeability of rock salt in WIPP underground facility. An in-situ experiment in performed to measure changes in brine and gas permeability of rock salt because of nearby excavation. The test intervals are isolated in the bottom monitoring boreholes with inflatable rubber packers, and initially pressurized to about 2 MPa. The formation pressure increases from near zero the pre-excavation. Injection tests a gradient of brine permeability from  $5 \times 10^{-18} \text{ m}^2$  (or to be estimated,  $10^{-5}$  Darcy) about the pre-excavation value  $10^{-21} \text{ m}^2$  (or  $10^{-9}$  Darcy).

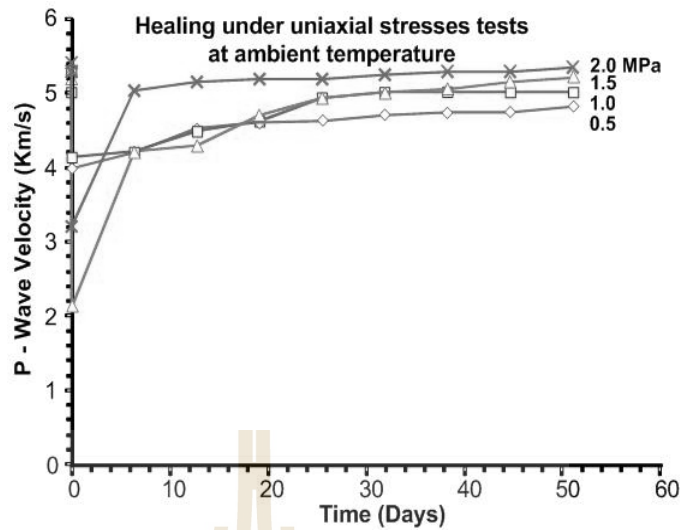


**Figure 2.6** P-wave velocities ( $H_e$ ) as a function of time ( $t$ ) of tension-induced fractures at uniaxial stresses 0.5 MPa. P-wave velocities ( $H_e$ ) as a function of time ( $t$ ) of tension-induced fractures at ambient temperature (Charoenpiew, 2015).

Stormont and Daemen (1992) conduct gas permeability and porosity measurements have been made during hydrostatic and triaxial quasi-static, stress-rate controlled compression tests. The permeability and porosity of the as-received samples decrease significantly because of hydrostatic loading. These changes are largely irreversible and are believed to “heal” or return the rock to a condition comparable to its undisturbed state. The permeability can increase more than 5 orders of magnitude over the initial (healed) state as the samples are deformed during deviatoric loading. The gas permeability and porosity changes are consistent with a flow model based on the equivalent channel concept. A model of micro crack initiation and growth based on the frictional sliding crack suggests the flow paths

initially develop along grain boundaries and then along axial intragranular tensile cracks. Post-test visual observations support the model predictions.

Peach (1991) develops a fundamental understanding of the influence of crystal plastic deformation on dilatancy and permeability evolution in salt rocks and salt/anhydrite rocks. It is experimentally based and seeks to explain the influence of deformation on permeability in the framework of "percolation theory", currently finding wide application in solid state physics. The results relate directly to the behavior of salt rock in disposal systems and, viewing salt as an analogue material, provide insight into the effects of plastic deformation on the fluid transport properties of crystalline rocks in general.

Houben et al. (2013) studied the micro cracks within the excavation damaged or disturbed zone (EDZ) in a salt-based radioactive waste repository (or an energy storage facility) can heal/seal by mechanical closure driven by compaction creep, by surface-energy-driven processes like diffusive mass transfer, and by recrystallization. It follows that permeability evolution in the excavation damaged zone around a backfilled or plugged cavity will in the short term be dominated by mechanical closure of the cracks, while in the longer-term diffusive mass transfer effects are expected to become more important. This studied is describes a contribution to assessing the integrity of radioactive waste repositories sited in rock salt formations by developing a microphysical model for single crack healing in rock salt. More specifically, single crack healing models for cracks containing a thin adsorbed water film are developed. These microphysical models are compared with single crack healing experiments, which conclusively demonstrate diffusion-controlled healing. Calibration of unknown model parameters, related to crack surface diffusivity, against

the experimental data enable crack healing rates under repository conditions to be estimated. The results show that after the stress re-equilibration that follows repository sealing, crack disconnection can be expected on a time scale of a few years at laboratory humidity levels. However, much longer times are needed under very dry conditions where adsorbed aqueous films are very thin.

Schulze et al. (2001) combined gas permeability with the P and S wave velocity measurements on rock salt samples from the Gorleben salt dome and the Morsleben salt mine under hydrostatic and triaxial loading conditions, mostly at room temperature. Permeabilities in the as-received samples vary between  $10^{-16}$  and  $2 \times 10^{-20}$  m<sup>2</sup>. The initial permeability is primarily due to decompaction induced by drilling, core retrieval and sample preparation. Hydrostatic loading gives rise to a marked decrease of permeability and a coeval significant increase of P and S wave velocities due to progressive closure of grain boundary cracks, tending to approach the in-situ matrix permeability ( $<10^{-20}$  m<sup>2</sup>). The pore space sensitivity of P and S wave velocities is used to monitor the in-situ state of the microstructure. Their reversals define the boundary in the state of stresses between dilatant and compactivity domains (dilatancy boundary). Dilatancy during triaxial deformation of the compacted rock salt samples is found to evolve stress dependent in various stages. The crack initiation stress increases from 18 MPa differential stress at 10 MPa confining pressure to 30 MPa at confining pressures above 70 MPa. Dilatancy is due to the opening of grain boundary and (100) cleavage cracks and depends on the applied confining pressure. The orientation of the open cracks is primarily controlled by the loading geometry system (compression, extension). As a consequence, permeability increases dramatically with progressive dilatancy, followed by a period

of plus/minus constant permeability during strain hardening up to 10% axial strain or even more. This suggests that the evolution of permeability is not only a function of dilatancy but also of microcrack linkage. Importantly, the anisotropic crack array within the samples causes a strong directional dependence of permeability.

Xiong et al. (2015) state that the damaged interfaces should be considered as main potential leakage path: firstly, in meso-level, gas flow rule along the interface is analyzed and the calculation of equivalent permeability is discussed. Then based on porous media seepage theory, gas leakage simulation model including salt rock, cavity interlayers and interface is built. With this strategy, it is possible to overcome the disadvantage of simulation burden with porous-fractured double medium. It also can provide the details of gas flowing along the damaged zones. Finally, this proposal is applied to the salt cavern in Qianjian mines. Under different operation pressures, gas distributions around two adjacent cavities are simulated; the evolvement of gas in the interlayers and salt rock is compared. From the results it is demonstrated that the domain of creep damage area has great influence on leakage range. And also, the leakage in the interface will accelerate the development of leakage in salt rock. It is concluded that compared with observations, this new strategy provides closer answers. The simulation result proves its validity for the design and reasonable control of operating pressure and tightness evaluation of group bedded salt rock storage caverns.

## **CHAPTER III**

### **SAMPLE PREPARATION**

#### **3.1 Introduction**

The objective of this chapter is to describe the sample preparation and simulation of tension-induced fractures and saw-cut surface of salt and potash specimens. The line load test is performed on the specimens to calculate healing effectiveness.

#### **3.2 Sample preparation**

The salt and potash specimens used in this study are obtained from the Middle salt and Lower salt members of the Maha Sarakham formation in the Khorat Basin, northeast of Thailand. The core specimens are from depths ranging between 200 and 400 m. The drilling is carried out by the ASEAN Potash Mining Co., Ltd. The tensile strengths of salt and potash are determined for designing the healing test parameters. The nominal dimensions of block specimens are shown in Table 3.1. The sample preparation and test procedures follow as much as practical the ASTM standard practices (i.e., ASTM D3967-95).

Two types of salt (Figure 3.1(a)) and potash (Figure 3.1(b)) fractures are simulated in the laboratory: 1) The line load method is used to simulate tension-induced fracture (Figure 3.2) given by axial load perpendicular to the specimens. The



load will be used to calculate the healing effectiveness from the tension-induced fracture (Table 3.2). 2) Saw-cut device is used to simulate the fractures formed by saw-cut surfaces (Figure 3.3). The potash specimens have carnallite contents ( $C\%$ ) varying from 80 to 90%, it can calculate in equation 3.1. Figure 3.4 shows specimens with tension-induced fracture (a) and saw-cut fracture (b) in the laboratory after fracture simulation.

$$C\% = [(\rho_s - \rho) / (\rho_s - \rho_c)] \cdot 100 \quad (3.1)$$

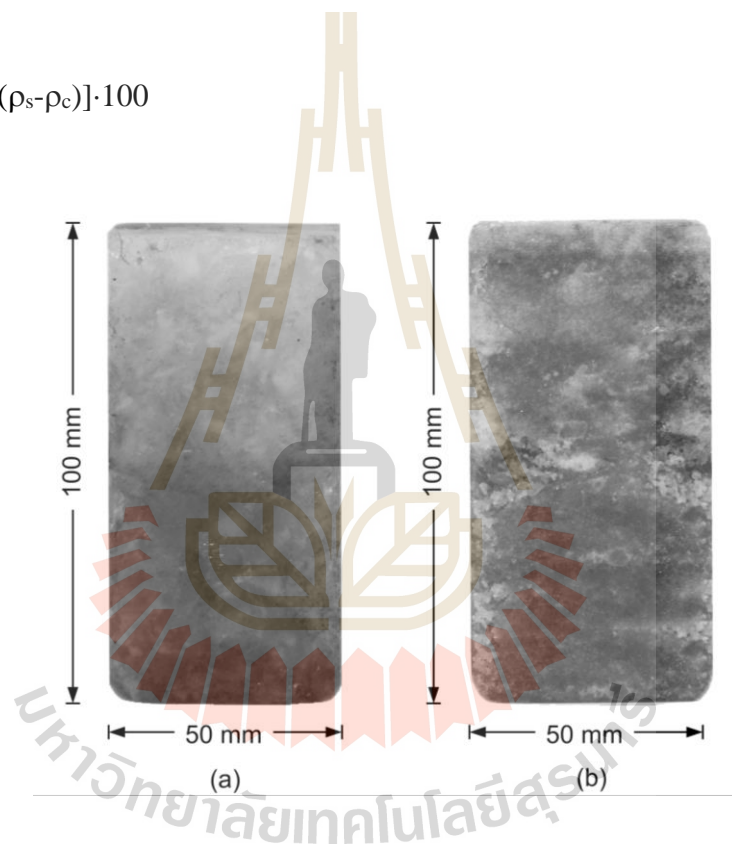


**Figure 3.1** Salt (a) and potash (b) specimens.



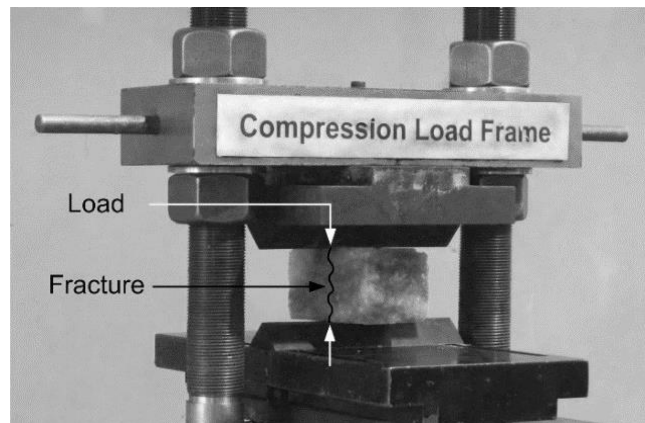


**Figure 3.2** Line load to induce tensile fracture.



**Figure 3.3** Saw-cut device.

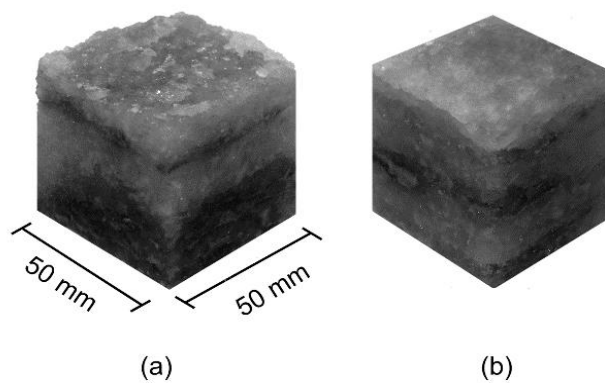


**Figure 3.4** Specimens with tensile fracture (a) and saw-cut surface (b).

**Table 3.1** Dimension of salt and potash specimens.

Sample	Specimen No.	Width (mm)	Length (mm)	Height (mm)	Density (g/cm <sup>3</sup> )	Carnallite contents (C%)
Salt	STF-01	49.24	50.11	99.98	2.13	0
	STF-02	49.44	49.83	99.91	2.14	0
	STF-03	50.04	49.56	99.86	2.14	0
	STF-04	49.76	49.93	99.93	2.15	0
	STF-05	50.08	50.03	99.91	2.14	0
	STF-06	49.62	49.98	99.62	2.13	0
	SSF-01	50.04	49.96	99.71	2.14	0
	SSF-02	50.03	49.95	99.65	2.11	0
Potash	PTF-01	49.21	50.04	98.98	1.65	82
	PTF-02	49.64	49.88	99.14	1.67	85
	PTF-03	49.83	49.88	99.68	1.68	83
	PTF-04	49.94	50.01	99.74	1.67	91

\*STF is salt tension-induced fractures

\*SSF is saw-cut surface

\*PTF is potash tension-induced fractures

# CHAPTER IV

## LABORATORY TEST AND RESULTS

### 4.1 Introduction

The objective of this chapter is explained the test method and test results. Tension-induced fractures of salt and potash are performs under various pressure at 21 days. The tests results are performed to study the effected of fractures type and pressure condition by using permeability to the index of fractures healing.

### 4.2 Test methods

A true triaxial load frame (Komenthammasopon, 2014) used to apply the constant axial and lateral stresses to the specimens (Figure 4.1a). All specimens are tests under ambient temperature (27°C). The healing tests are performed under the hydrostatic stresses ranging from 3, 5, 7, 10, 15 to 20 MPa for salt, and 5, 7, 10 to 15 MPa for potash. Saw-cut fractures are test only salt under stresses form 10 and 20 MPa. These stresses values are equivalent to in-situ stresses at depths ranging from 100 to 740 m.

Three pairs of 100-ton hydraulic pressure cylinders are set in three mutually perpendicular directions. The measurement system comprises pressure gauge (0-10,000 psi), displacement gauge (accuracy 0.01 mm), loading platen (50×50×60 mm) with L shaped hole ( $\phi = 5$  mm). The device can accommodate the cubic or rectangular specimens of different sizes by adjusting the distances between the opposite steel

loading platens. Neoprene sheets are placed at all interfaces between the loading platens, except around fracture. Before the line-load test are applied pressures under 5 days, for simulate the in-situ stresses. The fracture closure is monitored by dial gauges along the axial loading direction. They are continuously monitored every 2 hours for 21 days.

The nitrogen gas flow test (Figure 4.1b) is performed to measure the flow reduction of the fracture. The flow test system comprises of nitrogen gas tank, the flow meter, high-pressure tube and pressure regulator. Three gas flow meters used here are floating element type, which can measure the flow rates ranging from 10-100, 100-1000, and 1000-10,000 cm<sup>3</sup>/minute, limit under pressure equal to 60 psi. Nitrogen gas is injected under a constant pressure of 69 kPa (10 psi) through a high-pressure tube connected to the injection hole at the center of the loading platen (Figure 4.2). Gas flow tests have been performed every 12 hours throughout 21 days, and first day has been performed every 1 hours. The results are used to calculate the hydraulic aperture and intrinsic permeability of the fracture during healing. At the end of flow testing, the healed fracture is subjected to line-loading to assess the healing effectiveness. Line-loading are used as an indicator of the healing effectiveness. The test results are determined the healing effectiveness on healed fracture surfaces, compared tensile strength with intact rock specimen.

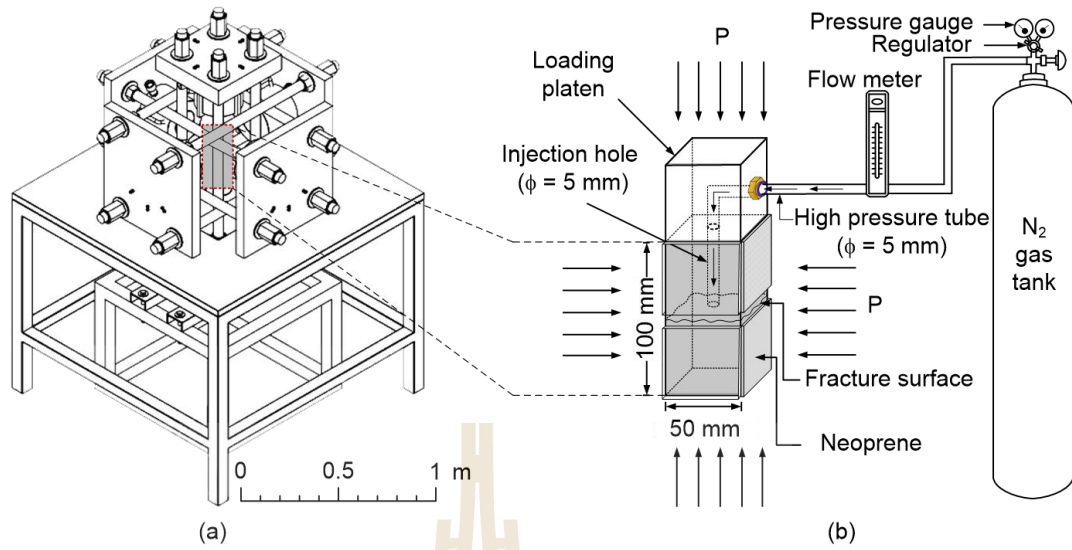


**Figure 4.1** True triaxial load device (a) and test specimen with drilled hole connected to nitrogen gas tank via high-pressure tube (b).

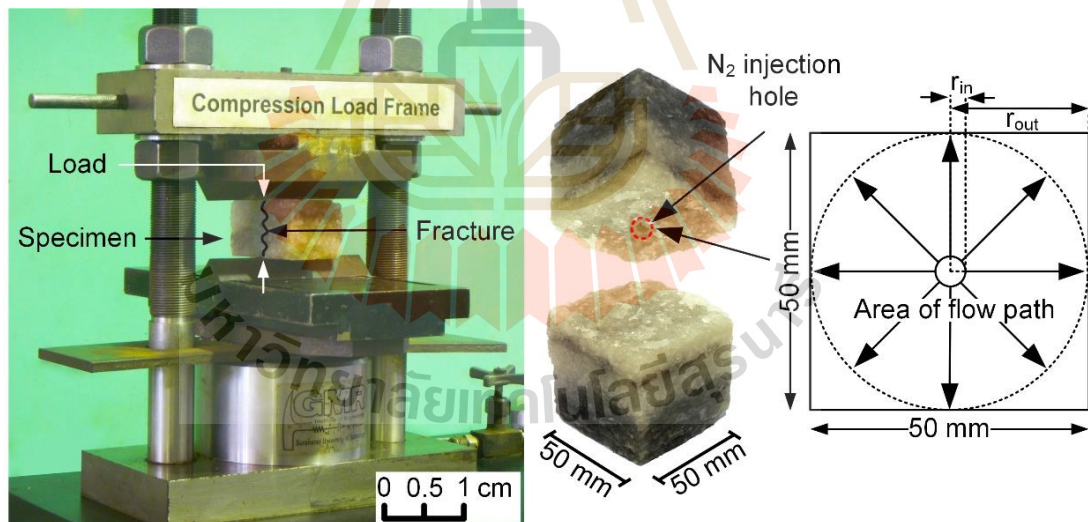


**Figure 4.2** Line load device and area of the radial flow path.

## 4.3 Test results

### 4.3.1 Hydraulic Properties

Figures 4.3 and 4.4 show the outflow rates as a function of time of tension-induced and saw-cut fractures. The flow rate reduction of the tension-induced fracture is affected by confining pressures and duration. It rapidly decreases during the first few day and tends to steadily drop through the end of the test. Under the same stress, fractures in potash show lower permeability than those in rock salt. Under 15 MPa, the flow rates reach the measurement limit of 10 cc/min within 13 days for salt and 3 days for potash. The flow rate of saw-cut surfaces remains unchanged.

The analytical solution to determine the permeability of the fracture is well-known as the “cubic law” which accurately describes flow for laminar flow between smooth-walled with a parallel plate (Boussinesq, 1868; Snow, 1970; Zeigler, 1976). However, natural fractures are more likely to be the rough surface, where the walls are contacting each other at discrete points (Gangi, 1978; Brown and Scholz, 1985; Brown and Hoek, 1978; Popp, 2012; Stormont, 1990).

The equivalent hydraulic aperture ( $e_h$ ) for the radial flow path is calculated by (Zeigler, 1976; Tsang and Witherspoon, 1981):

$$e_h = [6\mu_g \cdot Q \cdot \ln(r_{out}/r_{in}) / \pi\gamma_g(\Delta P)]^{1/3} \quad (4.1)$$

The intrinsic fracture permeability ( $k_i$ ) is calculated by (Zeigler, 1976):

$$k_i = e_h^2/12 \quad (4.2)$$

where  $\gamma_g$  is unit weight of nitrogen gas (11.428 N/m<sup>3</sup>),  $\mu_g$  is dynamic viscosity of nitrogen gas (1.759×10<sup>-5</sup> N·s/m<sup>2</sup>), Q is measured flow rate (m<sup>3</sup>/s),  $\Delta P$  is difference

between pressures injection and ambient pressures (psi),  $r_{in}$  radius of the injection hole, and  $r_{out}$  is equivalent in the outflow boundary.

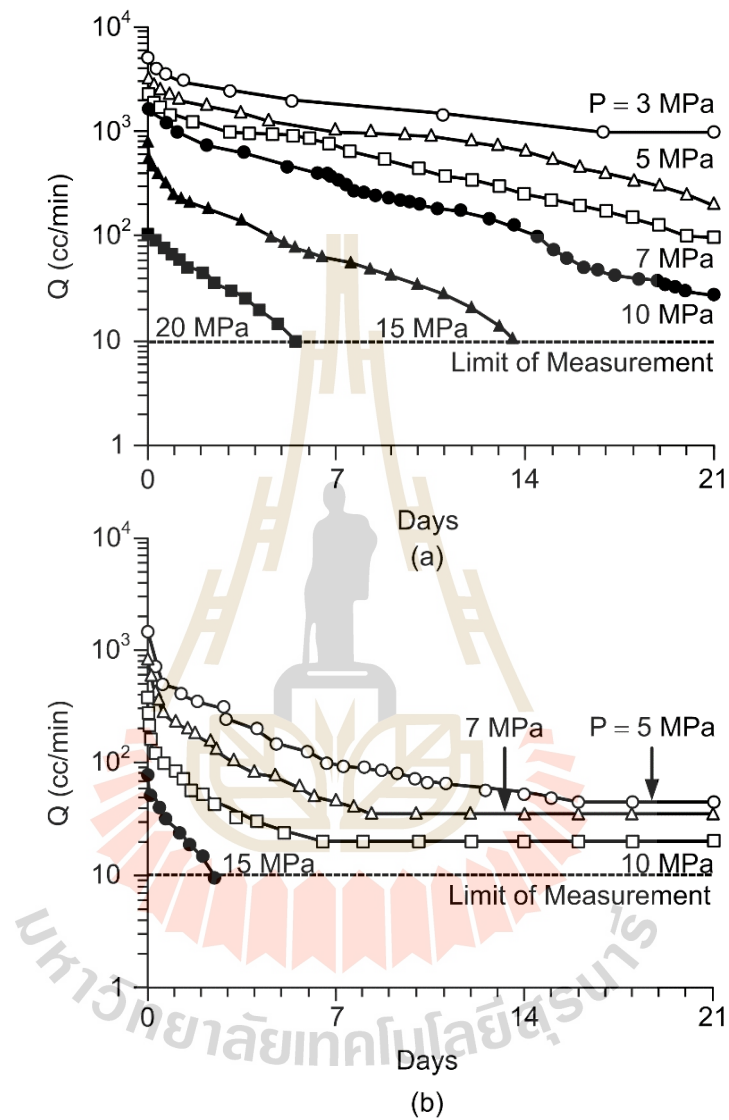


**Figure 4.3** Outflow rates ( $Q$ ) of tension-induced fractures in salt (a) and potash (b) as a function of time under various confining pressures ( $P$ ).



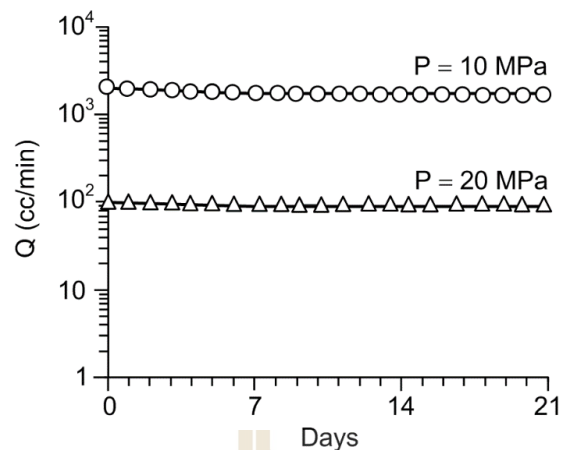


**Figure 4.4** Outflow rates ( $Q$ ) of saw-cut fracture in salt as a function time under various pressures ( $P$ ).

The results indicate that the hydraulic apertures of tension-induced fractures decrease with increasing pressure and duration, as shown in Figure 4.5. For saw-cut surface remains unchanged with increasing healing time. Note the hydraulic apertures can decrease several orders of magnitude with time.

Figures 4.6 and 4.7 show the intrinsic permeability as a function time of tension-induced and saw-cut fractures. The results indicate that the intrinsic permeability ( $k_i$ ) of tension-induced fractures decreases with increasing confining pressure and time. For saw-cut surface, the intrinsic permeability remains unchanged when increasing healing time.

### 4.3.2 Healing Effectiveness

The line load test results for intact and healed fractures are compared to assess the healing ability of the fractures. Figure 4.8 show healing of fracture after tests, the fracture can heal likely intact rock. Here the healing effectiveness represents the percentage of the failure load of healed fracture ( $F_h$ ) to failure load of intact



specimen ( $F_i$ ), as shown in Table 4.1. The results indicate that the healing effectiveness of salt and potash increase with increasing pressures as shown in Figure 4.9. It is found that healing has occurred in all fractures in salt and potash specimens after 21 days of pressurization. Recrystallization can be found only on the fractures in potash while the recrystallization in salt fracture is not noticeable. Under the same stresses fractures in potash specimens can heal quicker than those in salt specimens. Saw-cut fractures cannot efficiently heal, even under various pressure 10 and 20 MPa for 21 days.

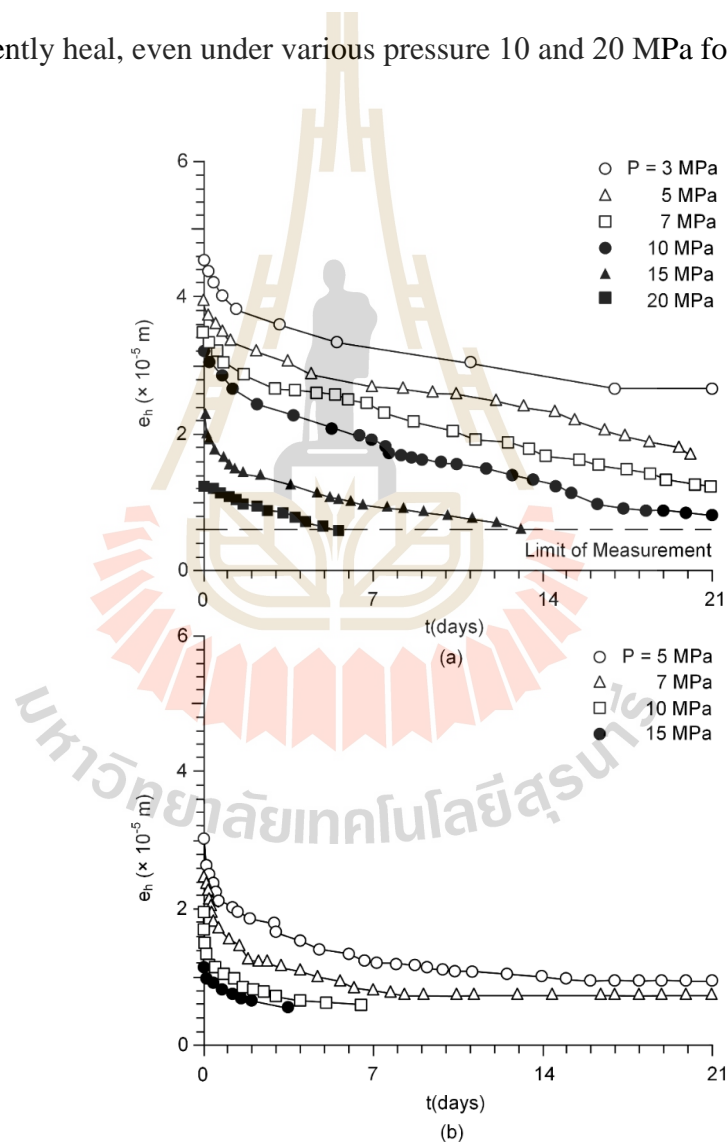


**Figure 4.5** Hydraulic apertures ( $e_h$ ) of tension induced fractures in salt (a) and potash (b) as a function time ( $t$ ).

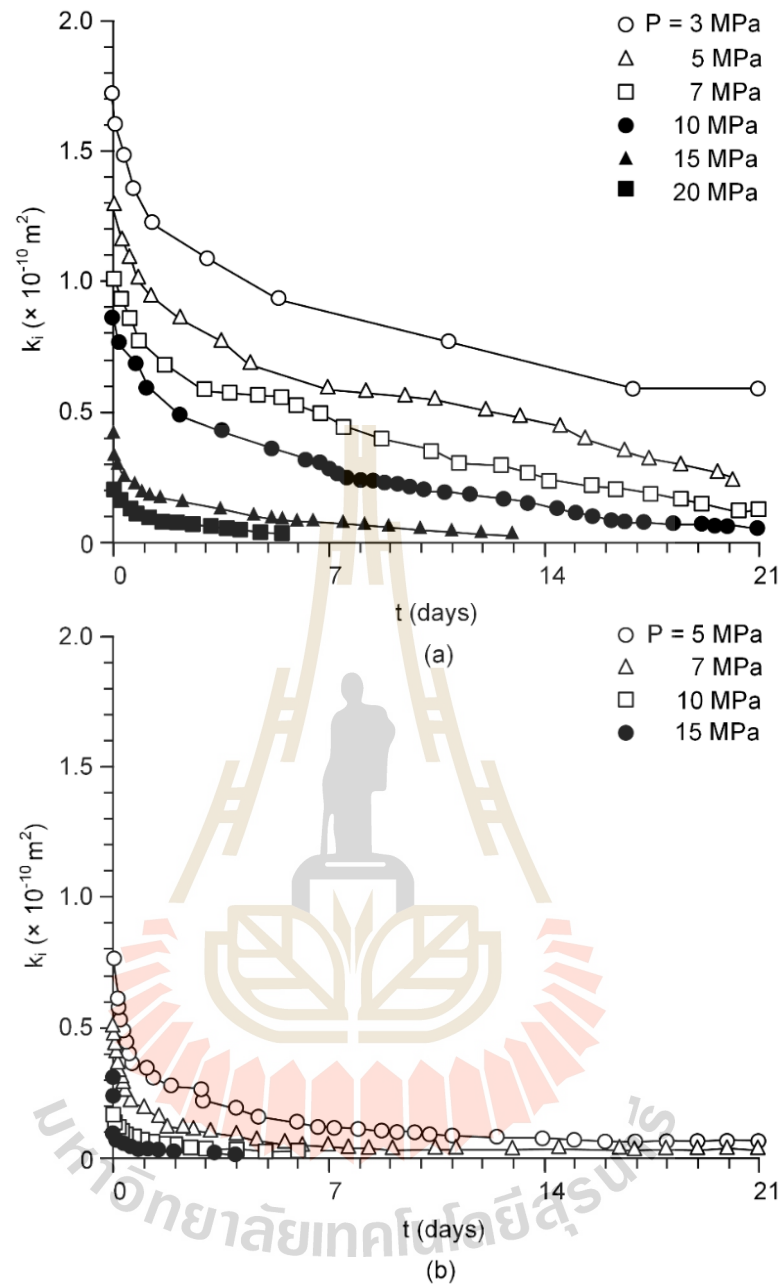


**Figure 4.6** Intrinsic permeability ( $k_i$ ) of specimens with tension-induced fractures in salt (a) and potash (b) as a function time under various confining pressures (P).

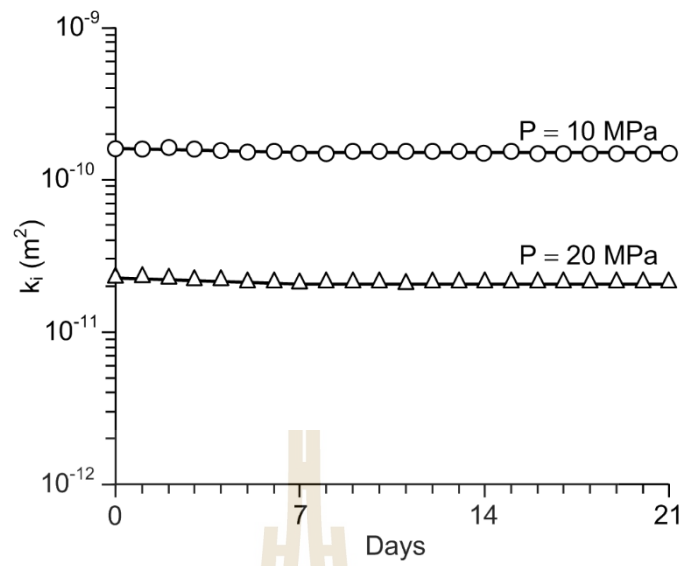


**Figure 4.7** Intrinsic permeability ( $k_i$ ) of specimens with saw-cut surface in salt as a function time under confining pressures ( $P$ ).

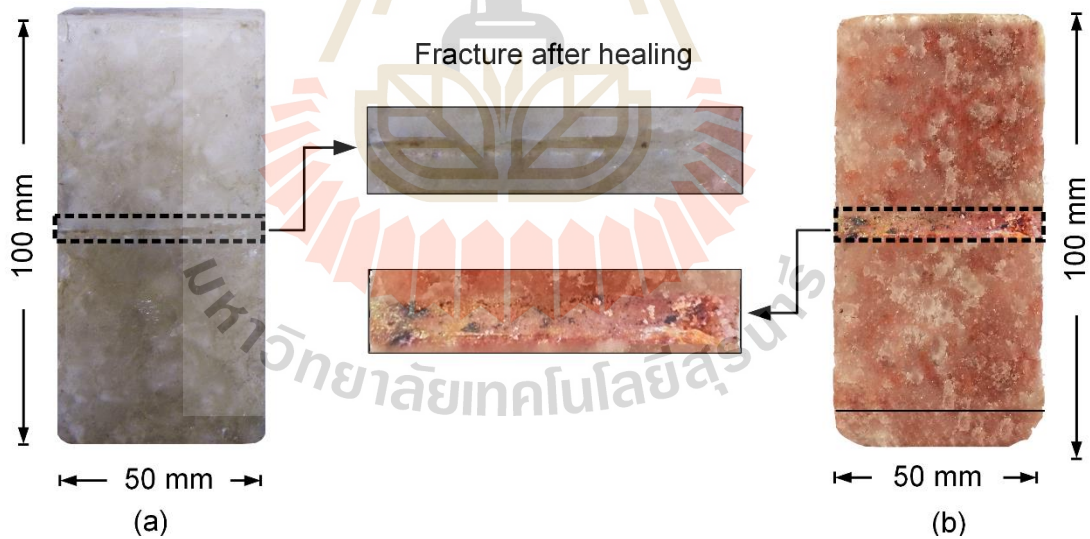


**Figure 4.8** Fractures healing after test of tension induced fracture in salt (a) and potash (b).

**Table 4.1** Line load test results of salt and potash specimens with tension-induced fractures and saw-cut surfaces after healing under confining pressures.

Sample No.	Series of testing	Confining pressure (MPa)	Line load test		Healing effectiveness $H_e = [F_h/F_i]$ (%)
			Intact salt, $F_i$ (kN)	Healed Fracture, $F_h$ (kN)	
STF-01	1	3	1.93	0.16	8.33
STF-02		5	1.99	0.37	18.62
STF-03		7	2.08	0.85	41.09
STF-04		10	2.26	1.25	55.36
STF-05		15	1.85	1.61	86.69
STF-06		20	2.05	1.85	90.20
SSF-01	2	10	1.87	0.00	0.00
SSF-02		20	1.96	0.00	0.00
PTF-01	3	5	0.27	0.06	20.08
PTF-02		7	0.29	0.17	56.90
PTF-03		10	0.21	0.16	76.39
PTF-04		15	0.32	0.30	91.55

$H_e = [\text{Failure load of healed fracture } (F_h) / \text{Failure load of intact } (F_i)] \cdot 100$  (%)

### 4.3.3 Strain Energy Principle

The strain energy principle is applied here to determine the energy required to heal the salt and potash fractures under different stresses and times. It is postulated that the fractures can be healed by applying the mean strain energy ( $W_m$ ). This energy can be calculated from the applied mean stresses and strains (Jaeger et al., 2007):

$$W_m = (3/2) \cdot \sigma_m \cdot \epsilon_m \quad (4.3)$$

$$\sigma_m = (\sigma_1 + \sigma_2 + \sigma_3) / 3 \quad (4.4)$$

$$\varepsilon_m = (\varepsilon_1 + \varepsilon_2 + \varepsilon_3)/3 \quad (4.5)$$

where  $\sigma_m$  is mean stress (MPa),  $\varepsilon_m$  is mean strain,  $\sigma_1$  is axial stress and  $\sigma_2$  and  $\sigma_3$  are lateral stresses. Note that the strain parallel to the fracture is equal to zero.

The results of salt and potash indicate that hydraulic aperture and intrinsic permeability decrease and healing effectiveness increase with increasing mean strain energy as shown in Figures 4.10, 4.11 and 4.12.

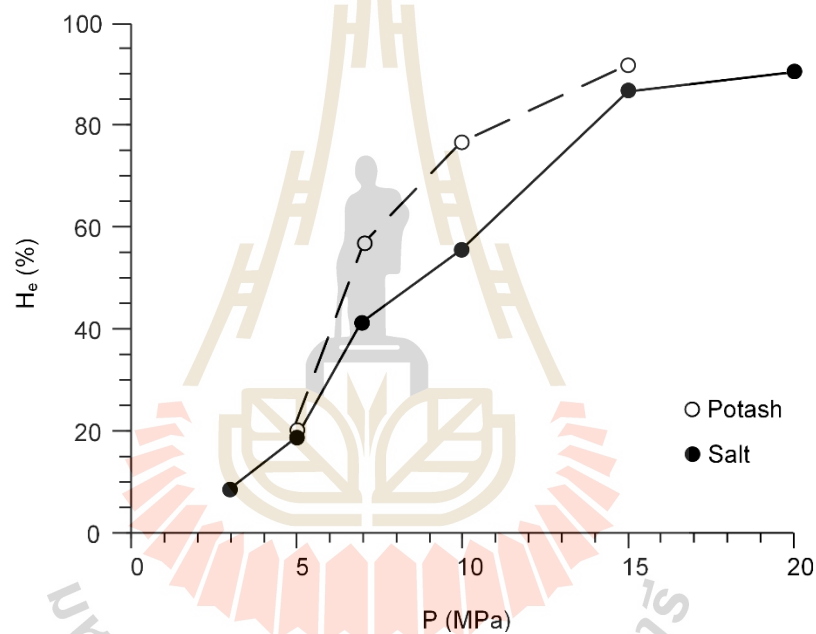


**Figure 4.9** Healing effectiveness ( $H_e$ ) of tension induced fracture in salt and potash as function time under various confining pressures.

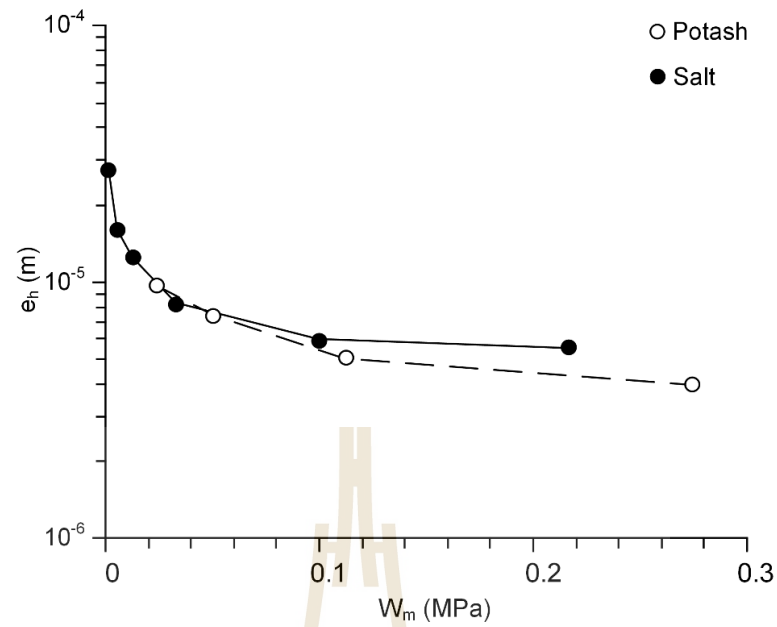


**Figure 4.10** Hydraulic aperture in salt and potash as a function mean strain energy.

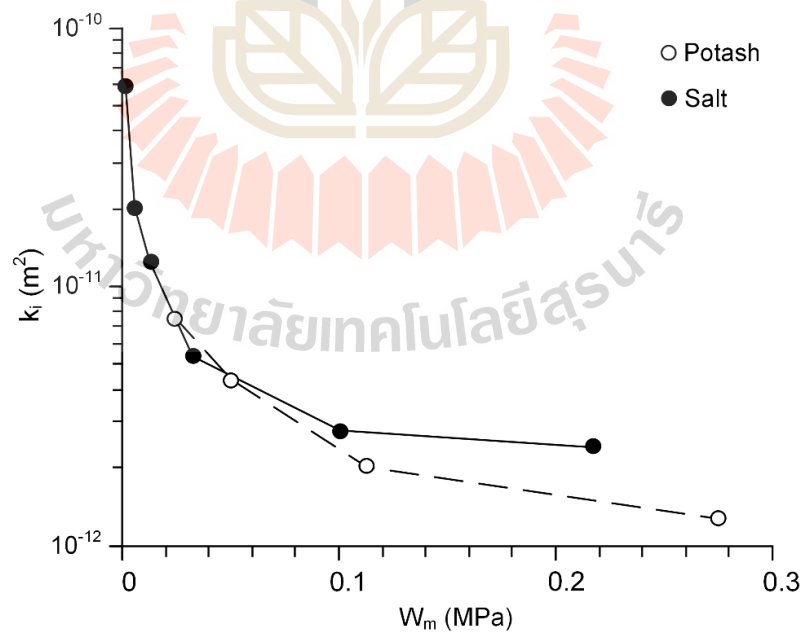


**Figure 4.11** Intrinsic permeability of salt and potash as a function mean strain energy.

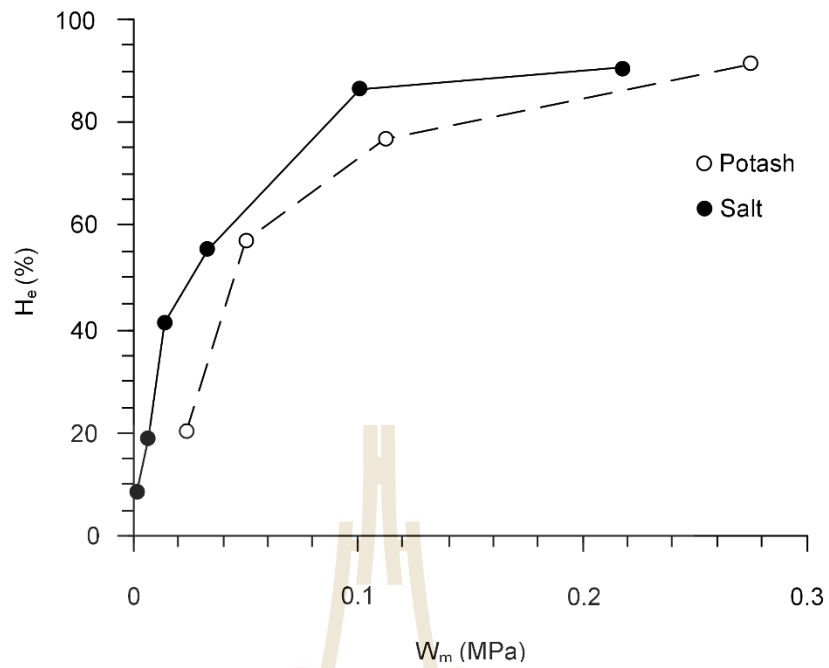


**Figure 4.12** Healing effectiveness in salt and potash as a function mean strain energy.

## CHAPTER V

### DERIVATION OF EMPIRICAL EQUATIONS

#### 5.1 Introduction

This chapter describes the development empirical equations linking the hydraulic aperture, intrinsic permeability and healing effectiveness as a function of pressure, time and means strain energy by using regression analyses (IBM SPSS Statistics 19, Colin and Paul, 2012). The relations are used to predict the healing of salt and potash fractures.

#### 5.2 Hydraulic properties

##### 5.2.1 Hydraulic aperture

The results indicate that the hydraulic aperture decrease with increasing confining pressure and time. Regression analysis of the test data (Figure 5.1) by SPSS software can determine the parameters of hydraulic aperture ( $e_h$ ) as a function of durations under applied pressures, as follows:

$$e_h = At^B \quad (5.1)$$

where A and B are functions of applied pressure for salt and potash which can be represented by:

$$A = \alpha P + \beta \quad (5.2)$$

$$B = \gamma P + \delta \quad (5.3)$$



where  $P$  is confining pressures (MPa),  $t$  is time (days),  $\alpha$ ,  $\beta$ ,  $\gamma$  and  $\delta$  are empirical constants, as shown in Table 5.1.

**Table 5.1** Empirical constants obtained for hydraulic aperture of salt and potash fracture as a function time under various pressures.

Parameters	Salt	Potash
$\alpha$	$-1.60 \times 10^{-6}$	$-1.81 \times 10^{-6}$
$\beta$	$4.35 \times 10^{-5}$	$3.20 \times 10^{-5}$
$\delta$	$-2.59 \times 10^{-2}$	$-1.10 \times 10^{-2}$
$\gamma$	$-4.17 \times 10^{-2}$	-0.362
$R^2$	0.922	0.938

### 5.2.2 Intrinsic permeability

Similar to the hydraulic aperture above the reduction of intrinsic permeability ( $k_i$ ) during the test can be determined by the regression analysis of the test data:

$$k_i = Ct^D \quad (5.4)$$

where  $C$  and  $D$  are functions of applied pressure which can be represented by:

$$C = \zeta P + \eta \quad (5.5)$$

$$D = \iota P + \kappa \quad (5.6)$$

where  $P$  is confining pressures (MPa),  $t$  is time (days),  $\zeta$ ,  $\eta$ ,  $\iota$  and  $\kappa$  are empirical constants, as shown in Table 5.2.

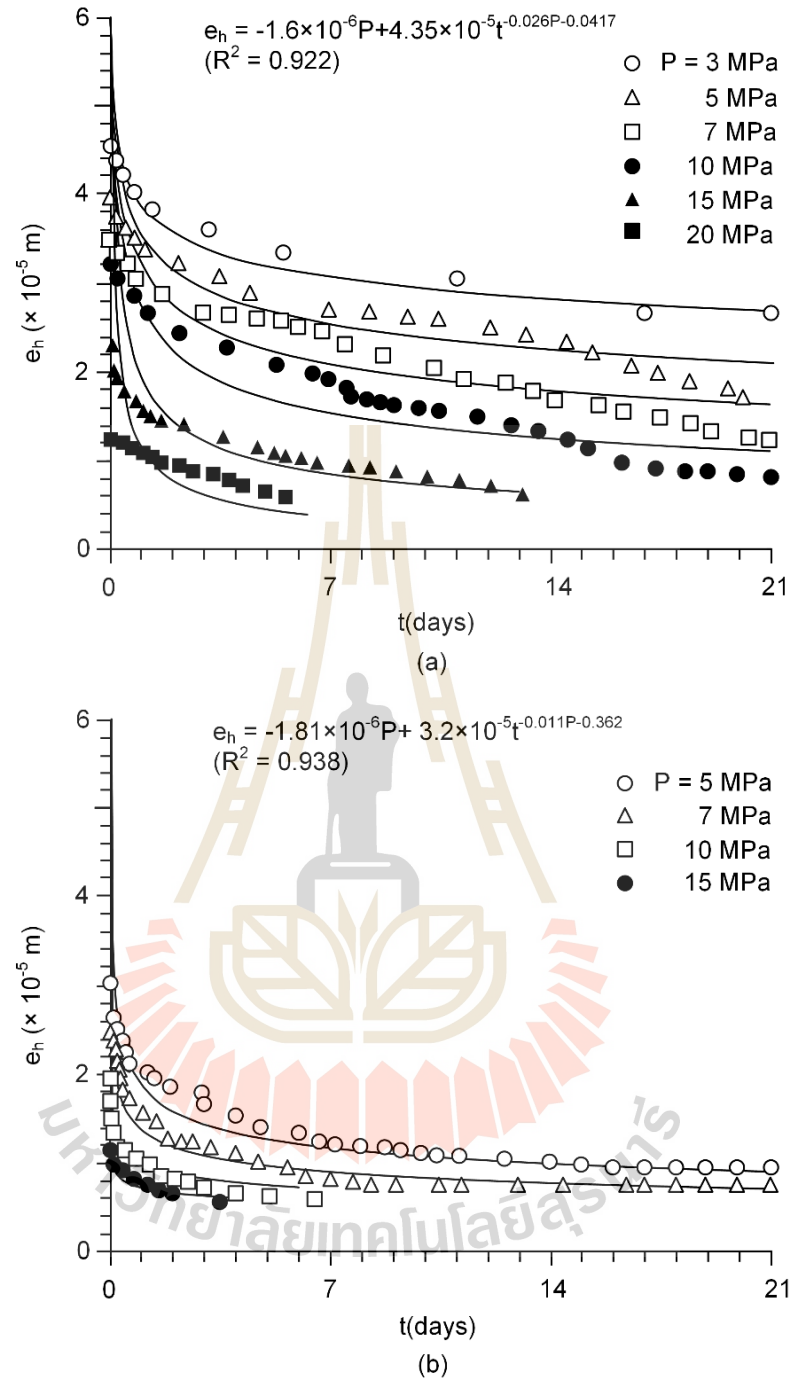


**Figure 5.1** Hydraulic aperture of salt (a) and potash (b) as a function of time under various pressures.

**Table 5.2** Empirical constants obtained for intrinsic permeability of salt and potash fractures under various pressures.

Parameters	Salt	Potash
$\zeta$	$-6.80 \times 10^{-12}$	$-4.23 \times 10^{-12}$
$\eta$	$1.40 \times 10^{-10}$	$5.96 \times 10^{-11}$
$\iota$	$-4.13 \times 10^{-2}$	$-2.22 \times 10^{-2}$
$\kappa$	-0.149	-0.586
$R^2$	0.927	0.943

### 5.3 Healing effectiveness

Healing occurs on all fractures in salt and potash fractures after 21 days. The line load test results of each specimen measured for intact and healed fractures are compared to assess the healing effectiveness. The relationship between healing effectiveness as a function of pressure curves can be represented by:

$$H_e = \tanh(\lambda P^\upsilon / 100) \quad (5.7)$$

where  $H_e$  is the healing effectiveness (%),  $P$  is the pressures (MPa),  $\lambda$  and  $\upsilon$  are empirical constants, as shown in Table 5.3. Figure 5.3 shows the healing effectiveness as a function of pressures. The results indicate that the healing effectiveness increases with increasing pressures. The healing effectiveness of fractures in potash specimens is higher than those of salt specimens under same the pressures. The predictions indicate that the healing effectiveness of fractures in salt and potash approach 100% after 21 days under pressures of 19.9 and 15.3 MPa, respectively.

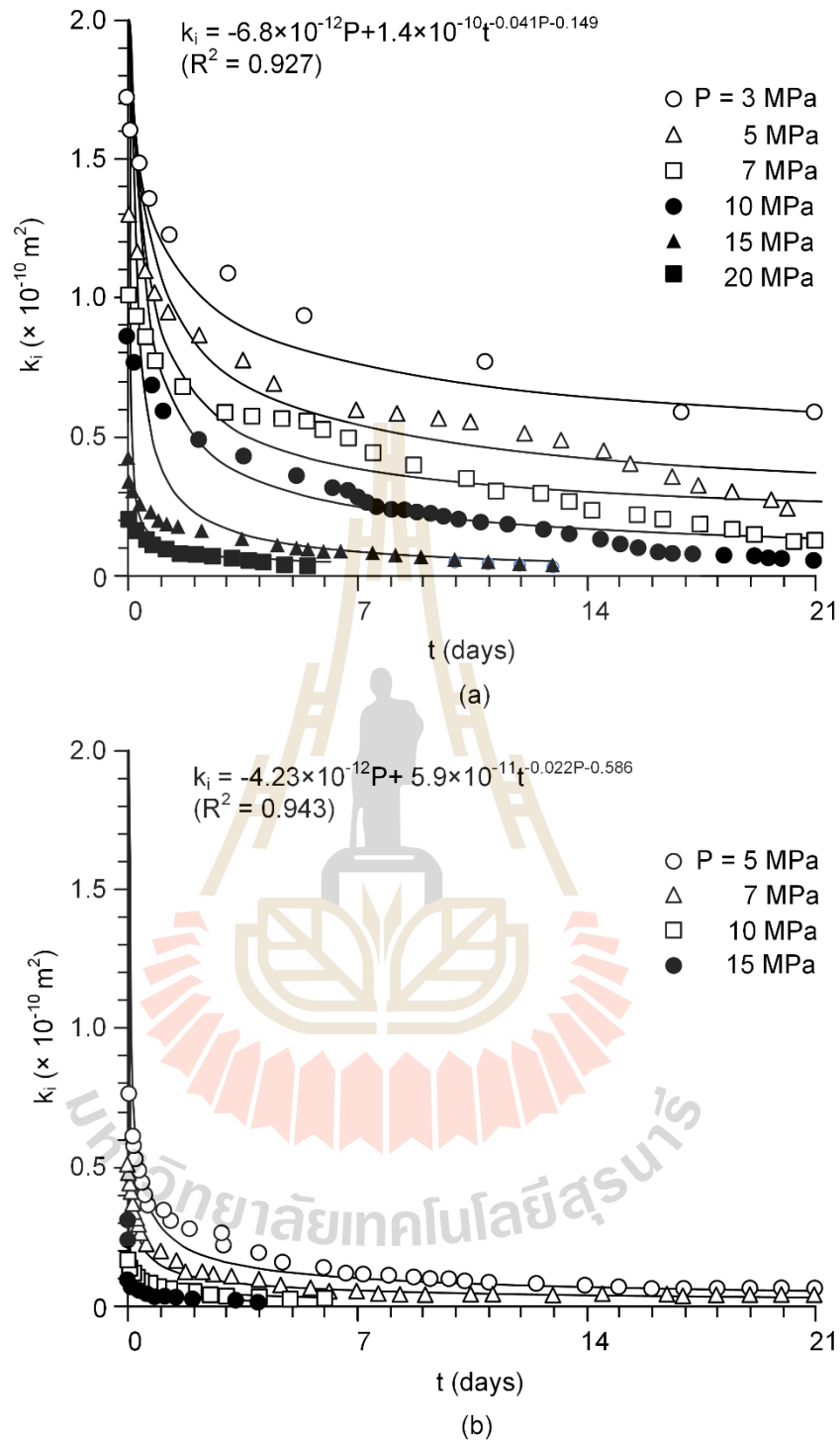


**Figure 5.2** Intrinsic permeability of salt (a) and potash (b) as a function time.

**Table 5.3** Empirical constants obtained for healing effectiveness of salt and potash fracture as a function pressure.

Parameters	Salt	Potash	Fuenkajorn&Phueakphum, 2011
$\lambda$	4.94	14.11	1.93
$\nu$	1.13	0.71	1.13
$R^2$	0.891	0.763	0.721

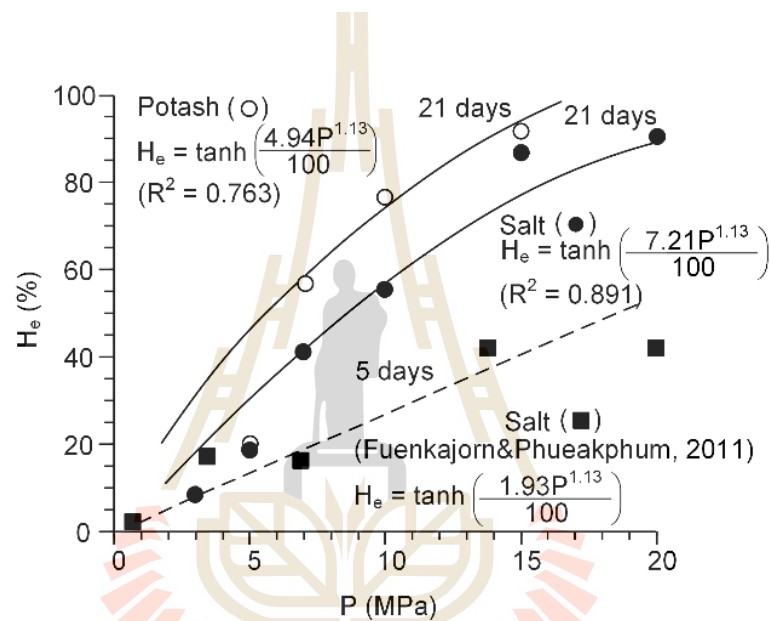


**Figure 5.3** Healing effectiveness of salt and potash as a function pressure.

The healing effectiveness of fractures in salt data as shown in Figure 5.3 obtained here and by Fuenkajorn and Phueakphum (2011) has been used to establish a mathematical relationship as a function of pressure and time. The healing effectiveness as a function of pressures and time can be represented by:

$$H_e = \tanh[P^\xi \cdot (\zeta t^{\tau P^0})] \quad (5.8)$$

where  $\xi$ ,  $\zeta$ ,  $\tau$  and  $\varphi$  are empirical constants, as shown in Table 5.4. Figure 5.4 shows the results, The healing increases with increasing duration under applied pressures. The mathematical relationships can be used to predict the mechanical properties of the healed fractures around openings as a function of time.

**Table 5.4** Empirical constants obtained for healing effectiveness of salt and potash fractures under various pressure as a function time.

Parameters	Values
$\xi$	1.13
$\zeta$	0.01
$\tau$	0.26
$\varphi$	0.31
$R^2$	0.732

#### 5.4 Mean strain energy

The strain energy principle is applied here to determine the energy required to heal the salt and potash fractures under different pressures and times. It is postulated that the fractures can be healed by applying the mean strain energy ( $W_m$ ). This energy can be calculated from the applied mean stresses and strains (Jaeger et al., 2007):  $W_m = (3/2) \cdot \sigma_m \cdot \varepsilon_m$ . where  $\sigma_m = (\sigma_1 + \sigma_2 + \sigma_3)/3$  and  $\varepsilon_m = (\varepsilon_1 + \varepsilon_2 + \varepsilon_3)/3$ ,  $\sigma_m$  is mean stress,  $\varepsilon_m$  is mean strain of fractures closure,  $\sigma_1$  is axial stress and  $\sigma_2$  and  $\sigma_3$  are lateral stresses. Note that the strain parallel to the fracture is equal to zero.

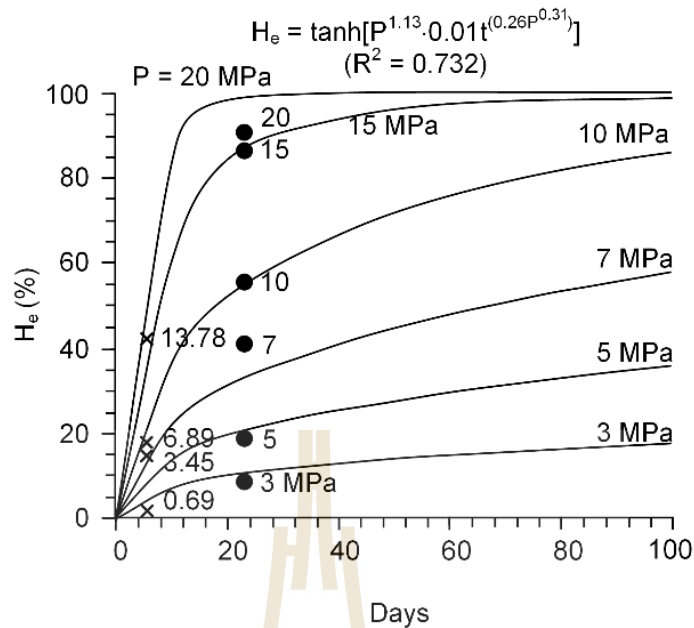


**Figure 5.4** Healing effectiveness with Fuenkajorn and Phueakphum (2011) as a function comparison times.

An attempt is made here to develop mathematical relationships between the hydraulic properties and the applied mean strain energy. Figure 5.5 shows the curve fits with the test results of the hydraulic aperture and mean strain energy. A power equation can describe the relation:

$$e_h = \chi \cdot W_m^\omega \quad (5.9)$$

where  $\chi$  and  $\omega$  are empirical constants, which are shown in Table 5.5. The empirical constants are obtained by regression analyses. Good correlations are obtained ( $R^2 > 0.9$ ).

**Table 5.5** Empirical constants obtained for hydraulic aperture of salt and potash fractures as a function means strain energy.

Parameters	Salt	Potash
$\chi$	$2.82 \times 10^{-6}$	$2.33 \times 10^{-6}$
$\omega$	-0.341	-0.372
$R^2$	0.981	0.988

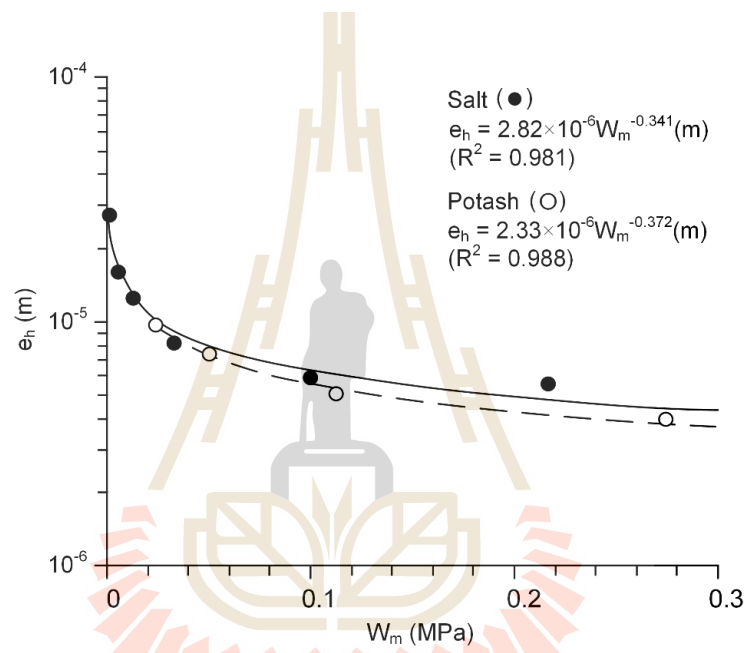


**Figure 5.5** Hydraulic aperture of salt and potash as a function mean strain energy.

Similar to the prediction above the reduction of intrinsic permeability during the test can be determined by the regression analysis of the test data. After several trials the variation of intrinsic permeability with mean strain energy can be best represented by a power relation:

$$k_i = \alpha' \cdot W_m^{\beta'} \quad (5.10)$$



where  $\alpha'$  and  $\beta'$  are empirical constants, which are shown in Table 5.6. Figure 5.6 show intrinsic permeability as a function of mean strain energy.

**Table 5.6** Empirical constants obtained for intrinsic permeability of salt and potash fractures as a function means strain energy.

Parameters	Specimens	
	Salt	Potash
$\alpha'$	$6.63 \times 10^{-13}$	$4.53 \times 10^{-13}$
$\beta'$	-0.681	-0.745
$R^2$	0.981	0.988

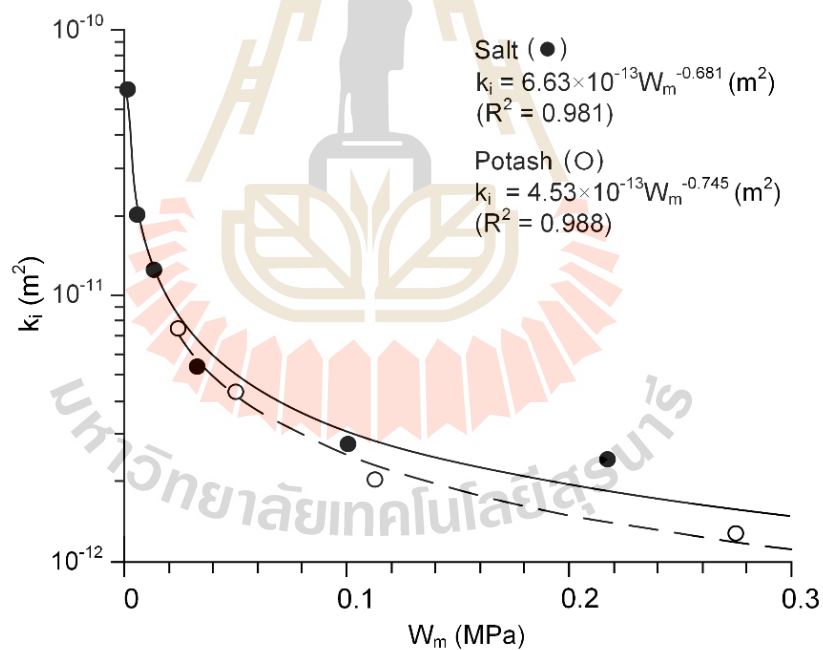


**Figure 5.6** Intrinsic permeability of salt and potash as a function mean strain energy.

An empirical equation is proposed to represent the healing effectiveness as a function of mean strain energy, as follows:

$$H_e = 100 \cdot \tanh(\gamma' W_m^{\delta'} / 100) \quad (5.11)$$

where  $\gamma'$  and  $\delta'$  are empirical constants, which are shown in Table 5.7. The correlation coefficients are greater than 0.9. Figure 5.7 shows the test results fitted with hyperbolic function. It should be noted that the prediction of healing effectiveness as a function of time cannot reach 100%. The relations can be used to predict the hydraulic properties of rock salt and potash fractures around the borehole under various external pressures. The opening depth and time at which the sealing are significant factors controlling its long-term hydraulic properties.

**Table 5.7** Empirical constants obtained for healing effectiveness of salt and potash fractures as a function means strain energy.

Parameters	Specimens	
	Salt	Potash
$\gamma'$	398	460
$\delta'$	0.51	0.72
$R^2$	0.989	0.927

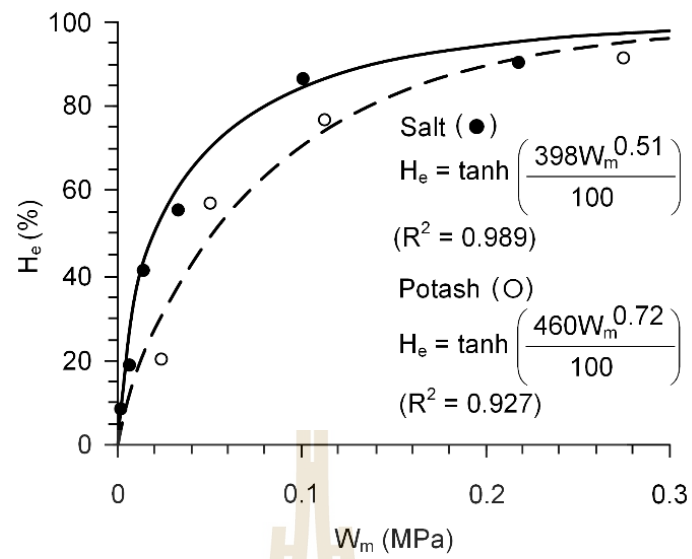


**Figure 5.7** Healing effectiveness of salt and potash as a function mean strain energy.



# CHAPTER VI

## DAMAGE RECOVERY

### 6.1 Introduction

The objective of this chapter is to predict the hydraulic and mechanical performance of fractures in rock salt and potash around boreholes after sealing. The time-dependent closure of borehole is calculated in terms of the released mean strain energy. The salt and potash fracture performance are predicted for different opening depths and sealing periods.

### 6.2 Borehole in salt and potash mass subjected to uniform external pressure

The mean strain energy released by creep closure of borehole in infinite salt and potash masses subjected to uniform external pressure (in situ stress) is used to correlate opening with the hydraulic aperture, intrinsic permeability and healing effectiveness around wall after sealing. The released energy ( $W_m$ ) can be calculated from the stresses and strains at the borehole wall as:

$$W_m = (3/2) \cdot [(\sigma_r + \sigma_\theta + \sigma_z)/3] \cdot [(\varepsilon_r + \varepsilon_\theta + \varepsilon_z)/3] \quad (6.1)$$

where  $\sigma_r$ ,  $\sigma_\theta$  and  $\sigma_z$  are radial, tangential and axial stresses and  $\varepsilon_r$ ,  $\varepsilon_\theta$  and  $\varepsilon_z$  are radial, tangential and axial strains.

Under plane strain condition the radial and tangential stresses obtained from the Kirsch's solution can be presented (Jaeger et al., 2007) as:

$$\sigma_r = [1 - (a^2/r^2)] \cdot P_o \quad (6.2)$$

$$\sigma_\theta = [1 + (a^2/r^2)] \cdot P_o \quad (6.3)$$

where  $P_o$  is external pressure,  $a$  is borehole radius and  $r$  is radial distance from the center. The axial stress ( $\sigma_z$ ) can be calculated by poisson ratio ( $\nu$ ):

$$\sigma_z = \nu (\sigma_r + \sigma_\theta) \quad (6.4)$$

At the borehole wall, the strains are defined as:

$$\varepsilon_r = \varepsilon_r^e + \varepsilon_r^c \quad (6.5)$$

$$\varepsilon_z = \varepsilon_\theta = 0 \quad (6.6)$$

where  $\varepsilon_r^e$  is the elastic radial strain and  $\varepsilon_r^c$  is the time-dependent radial strain controlling the creep closure of the borehole.

The elastic radial strain can be obtained by (Jaeger et al., 2007):

$$\varepsilon_r^e = 1/E [(1 - \nu^2)\sigma_r - \nu(1 + \nu)\sigma_\theta] \quad (6.7)$$

Nair and Boreisi (1970), and Fuenkajorn and Daemen (1988) have derived the radial creep strain around circular hole based on the potential creep law and the associated flow rule as:

$$\varepsilon_r^c = 3/2 \kappa_b (\sigma^*)^{(\beta_b - 1)} \cdot S_r (t_1^{\gamma_b} - t_0^{\gamma_b}) \quad (6.8)$$

where  $\kappa_b$ ,  $\beta_b$  and  $\gamma_b$  are material constants of the potential creep law,  $S_r$  is the radial stress deviation,  $\sigma^*$  is the equivalent (effective) stress,  $t_0$  is time at which loading is

applied (usually assumed to be zero) and  $t_1$  is time at which the strains are calculated.

The stress deviation can be obtained from:

$$S_r = \sigma_r - (\sigma_r + \sigma_\theta + \sigma_z)/3 \quad (6.9)$$

$$\sigma^* = 1/\sqrt{2} [(\sigma_r - \sigma_\theta)^2 + (\sigma_\theta - \sigma_z)^2 + (\sigma_z - \sigma_r)^2]^{1/2} \quad (6.10)$$

Substituting Equation (6.2) - (6.10) into Equation (6.1) the released mean strain energy (by closure) at the borehole wall can be calculated. To demonstrate the application of the strain energy concept used here, the mechanical and rheological parameters of salt and potash (80% carnallite) obtained from Wilalak and Fuenkajorn (2016) are assigned to the equation 6.8, where  $\kappa_b = 3 \times 10^{-4}$  1/MPa · day,  $\beta_b = 1.358$  and  $\gamma_b = 0.194$  for rock salt and  $\kappa_b = 2.31 \times 10^{-3}$  1/MPa · day,  $\beta_b = 1.414$  and  $\gamma_b = 0.246$  for potash. The elastic parameters of rock salt and potash are obtained from Luangthip et al. (2016) who report that the elastic modulus (E) and Poisson's ratio ( $\nu$ ), are equal to 4.2 GPa, 0.27 for rock salt, and 18.87 GPa, 0.38 for potash. The released energy at the borehole wall is calculated from the external pressures at depth of 200, 250 and 300 m (equivalent to the pressure approximately of 4.51, 5.56 and 6.63 MPa). Figure 6.1 plots the released strain energy ( $W_m$ ) as a function of time after drilling. The mean strain energy increases rapidly, particularly during the first year. The rate of releasing energy reduces with time. The greater external pressures (deeper borehole) lead to the larger released energy. The diagrams suggest that the time at which sealing ( $t_s$ ) is a significant factor dictating the amount of released energy remaining for hydraulic and mechanical performance of the fractures.

### 6.3 PREDICTION OF SALT AND POTASH AFTER SEALING

Predicting the hydraulic aperture, intrinsic permeability and healing effectiveness in salt and potash around borehole after sealing, the strain energy left for the healing is needed. It can be obtained from:

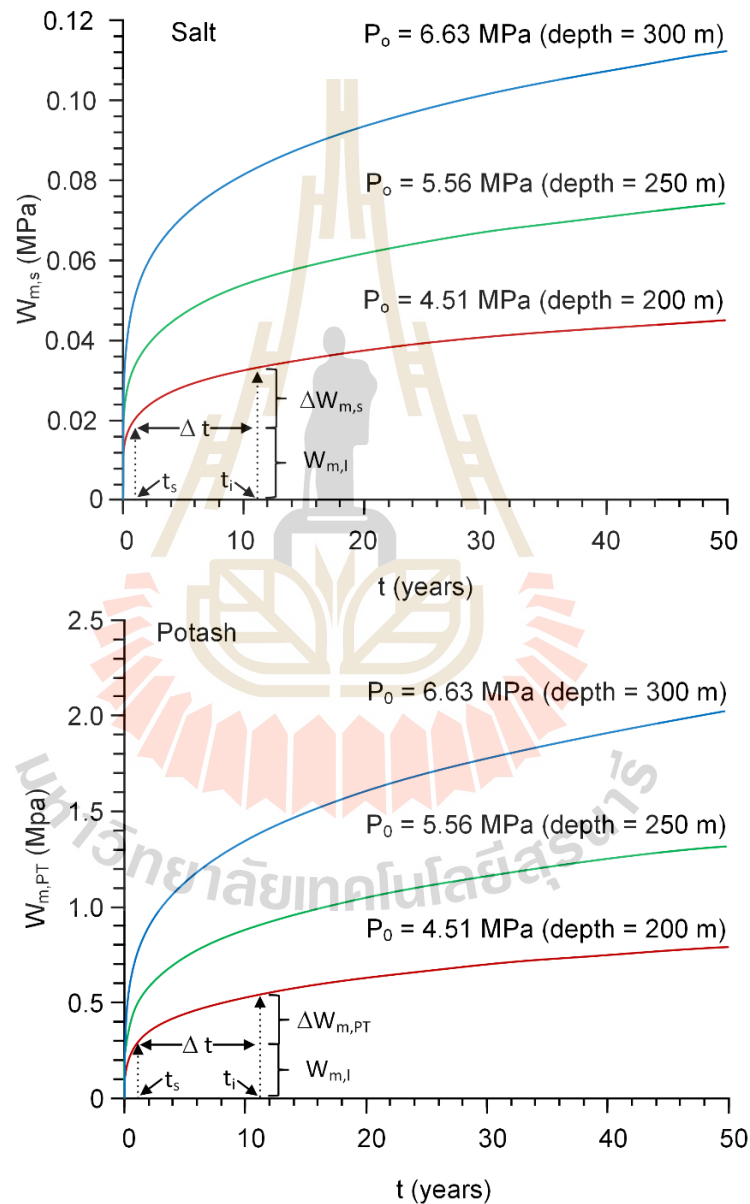


**Figure 6.1** Release mean strain energy of borehole closure in salt and potash as a function of times.

$$\Delta W_m = W_{m,r} - W_{m,l} \quad (6.11)$$

where  $W_m$  is the total released energy from drilling to any selected period ( $t_i$ ) determined as if no borehole sealing, and  $W_{m,l}$  is the energy lost due to creep closure before sealing. The time at which sealing is designated as  $t_s$  in Figure 6.1 The duration of healing ( $\Delta t$ ) can be obtained from:

$$\Delta t = t_i - t_s \quad (6.12)$$

The  $\Delta W_m$  at depths of 200, 250 and 300 m are calculated for  $t_s = 1, 2$  and 3 years. The prediction period ( $\Delta t$ ) is up to 50 years after sealing. From Equation (6.11)  $\Delta W_m$  can be calculated as a function of  $\Delta t$ , as shown in Figure 6.2. The results indicate that the  $\Delta W_m$  increase with increasing time ( $\Delta t$ ). This is because the released energy by creep closure of the borehole after sealing is contributed by the increase of the radial stresses and the decrease of the radial strain rate at the borehole boundary. This is caused by the mechanical interaction between the borehole wall and the sealing. The effect of  $t_s$  is more pronounced under high  $P_o$  than under low  $P_o$ . This implies that the time at which the sealing is more critical for deep borehole than for the shallow ones.

Substituting  $\Delta W_m$  and  $\Delta t$  values from Figure 6.2 into  $W_m$  in chapter V equations (5.9) to (5.11) the hydraulic aperture, intrinsic permeability and healing effectiveness can be predicted, as shown in Figures 6.3, 6.4 and 6.5. For this demonstration, the predictions are made up to 50 years. The results suggest that the hydraulic aperture and intrinsic permeability decreases, and healing effectiveness increases with increasing time ( $\Delta t$ ). The effects of sealing time ( $t_s$ ) on the hydraulic aperture, intrinsic



permeability and healing effectiveness are more pronounced after in deep borehole than in shallow ones.

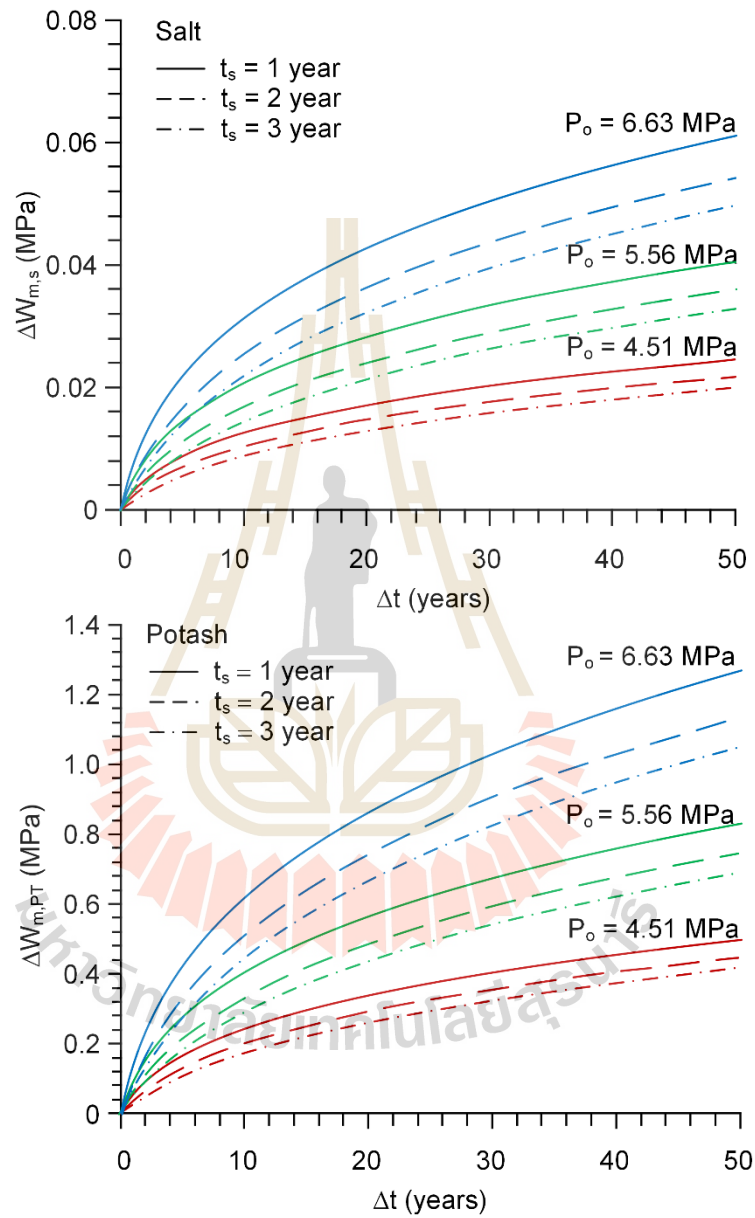


**Figure 6.2** Remaining mean strain energy ( $\Delta W_m$ ) as a function of time after sealing.

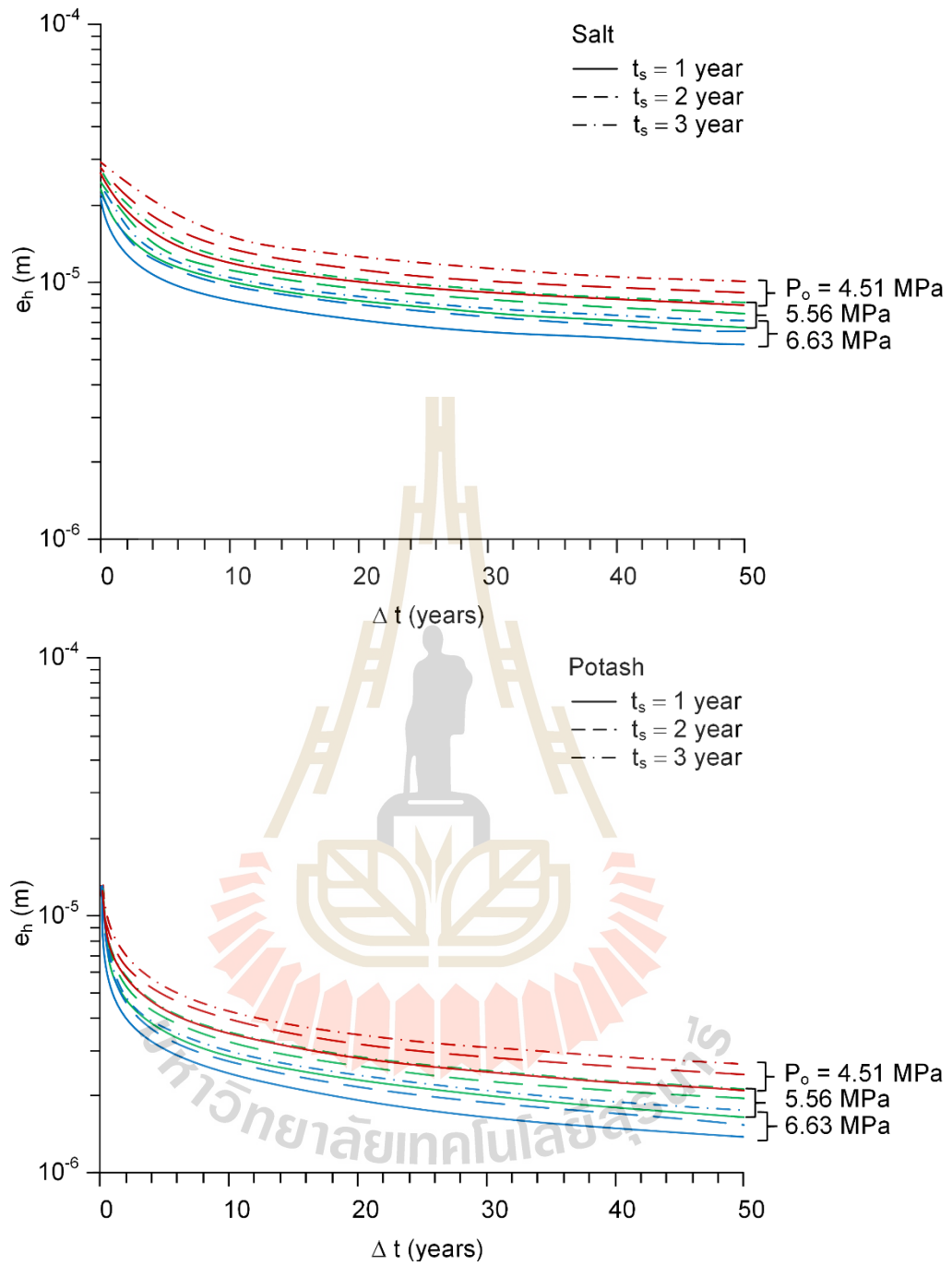


**Figure 6.3** Hydraulic aperture ( $e_h$ ) of salt and potash as a function time after sealing.

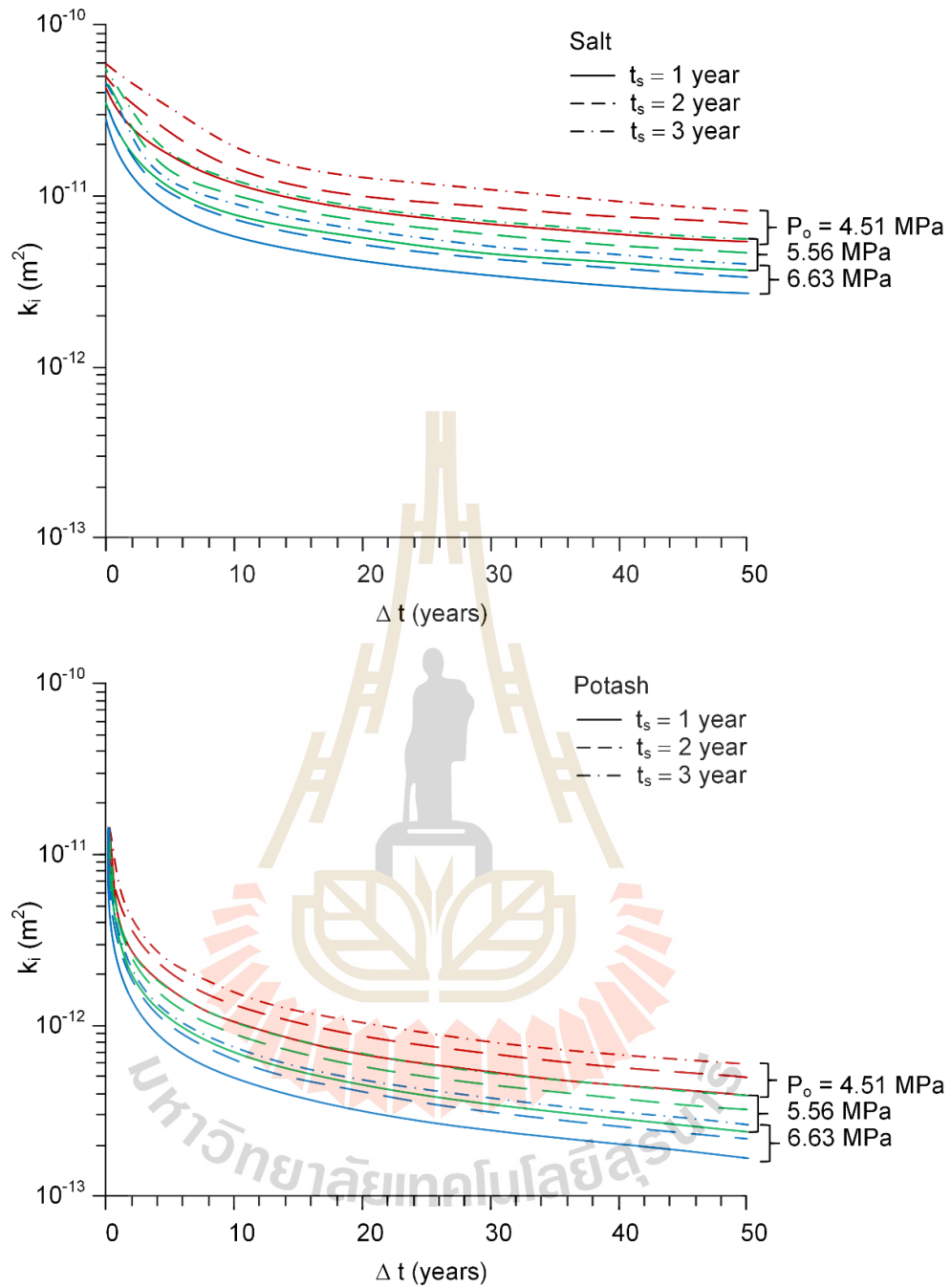


**Figure 6.4** Intrinsic permeability ( $k_i$ ) of salt and potash as a function time after sealing.

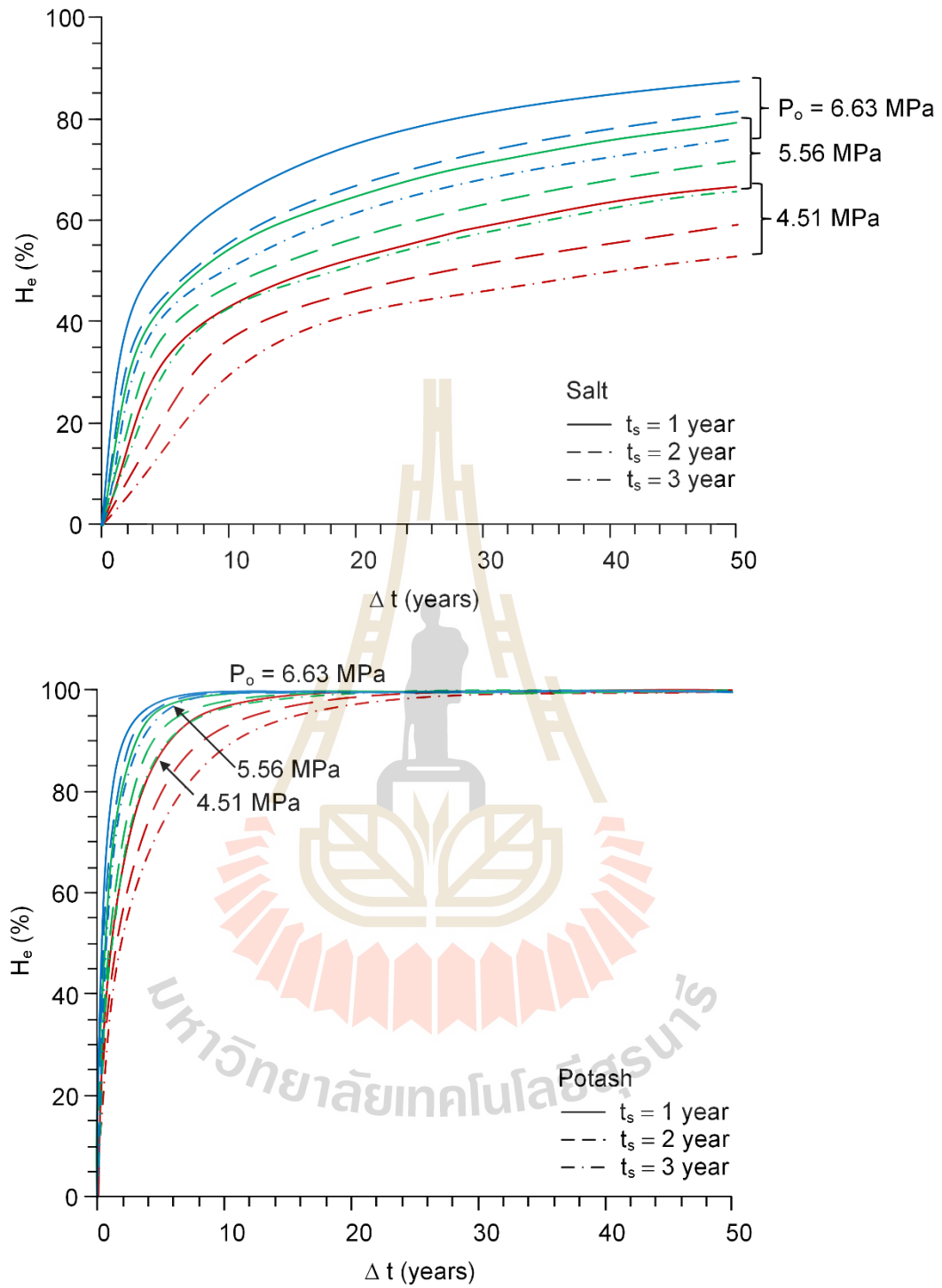


**Figure 6.5** Healing effectiveness ( $H_e$ ) of salt and potash as a function time after sealing.

# **CHAPTER VII**

## **DISCUSSIONS, CONCLUSIONS AND RECOMMENDATIONS FOR FUTURE STUDIES**

### **7.1 Discussions**

This section discusses the key issues relevant to the reliability of the test schemes and the adequacies of the test results. The objective of this research is to experimentally determine the healing of salt and potash fractures under long-term and various confining pressures. This thesis described the detailed test methods, empirical regression parameters and predicted hydraulic and mechanical performance around opening after sealing in salt and potash mines.

A total of 8-salt and 4-potash fracture specimens have been assessed for the healing effectiveness under various pressures for 21 days. The test is under long-term as compared to the experimental work performed on fractures healing elsewhere (Fuenkajorn and Phueakphum, 2011; Charoenpiew, 2015). The results tend to be reliable, as evidenced by the overlapping (repeating) of the healing effectiveness under various pressures with the same duration.

1) The pressure conditions of tension-induced fractures are under hydrostatic stresses ranging from 3 to 20 MPa for rock salt and 5 to 15 MPa for potash. The results indicate that the healing effectiveness increase with hydrostatic stresses. These results generally agree with those of Fuenkajorn and Phueakphum (2011) and Charoenpiew (2015). Hydrostatic stresses can heal fracture better than the radial load under same

pressure condition. It is postulated that the fracture can be expand in the no bound direction, and hence the contact area of fractures can affect the healing process.

2) The durations increase the healing effectiveness and decrease intrinsic permeability and hydraulic aperture. The durations are an important factor in the healing of fracture process. These results agree well with those of Fuenkajorn and Phueakphum (2011) and Charoenpiew (2015). The healing effectiveness at 21 days are higher than at 5 days (Fuenkajorn and Phueakphum, 2011), as healing process does not occur immediately after fracture closure. The healing mechanism by recrystallization and covalent bonding are dependent of duration.

3) Permeability is important index to explain fracture healing behavior under various pressures in long-term. The results indicate that hydraulic aperture and intrinsic permeability decrease with increasing pressure and time. The results agree well with Fuenkajorn and Phueakphum (2011). They rapidly decrease during the first few days and tend to steadily drop through the end of the test. Under the same pressure, fractures in potash show lower permeability than those in rock salt. The elastic modulus has an effect on fracture closure (elastic of potash is lower than salt). The influences of elastic modulus on the fracture closure are reflected as the reduction of intrinsic permeability and hydraulic aperture.

4) Fracture types in this study are tension-induced fractures and saw-cut surfaces. The results indicate that saw-cut fracture cannot be healed. Tension-induced fracture can heal due to covalent bonding between cleavage which agrees well with the conditions drawn by Fuenkajorn and Phueakphum (2011). This is supported by the fact that the cleavage planes in the salt crystal are purer than the inter crystalline boundaries. and purer than the saw-cut surfaces. The saw-cut surfaces could be contaminated during

the preparation process.

5) As evidenced by the good correlation coefficients ( $R^2 > 0.8$ ) obtained from the proposed empirical equation, the test results are reasonably reliable. This is true for all testing: permeability and healing effectiveness test results. It is however not intention here to claim that the proposed empirical form of the hydraulic and mechanical empirical is universally applicable to all fracture characteristics. The proposed equation, however, has an obvious advantage that it can represent the behavior of fracture healings in salt and potash.

## 7.2 Conclusions

All objectives and requirements of this study have been met. The results of the laboratory testing and analyses can be concluded as follows:

1) The healing effectiveness increases with increasing pressures and time. Under the same pressures and time, fractures in potash specimens can heal quicker than those in salt specimens. The fracture healing depends on healing mechanisms (covalent bonding and recrystallation processes), pressurization and duration. The healing effectiveness of fractures in potash (recrystallation process) is higher than the fractures in salt (covalent bonding). This suggests that healing by recrystallation process maybe more effective than by covalent bonding between the two surfaces.

2) Two main mechanisms simultaneously occur (1) the healing process and fracture closure and (2) covalent bonding and recrystallization. Both can improve fracture healing, and the mechanical and hydraulic performance of the healed fractures. The pressures and duration have a great effect on the fractures healing in salt and potash, possibly due to the contact area contact of fracture heal. It is postulated that the fracture

healing increases with increasing fracture closure, and hence promoting covalent bonding and recrystallization within the boundaries of fractures.

3) Fracture permeability obtained from the flow testing can be derived as a function of the applied mean strain energy. This allows predicting of the salt and potash fractures around openings, providing that the mean stress and strain of the fracture closure are known. The mean stress is related to the depth where the fractures are developed. This suggests that fractures at greater depth may reduce permeability quicker than those at shallower depth. Similarly, the healing effectiveness also increases with mean strain energy, as suggested by the diagram in Figure 5.7. Under the same mean strain energy, the salt fractures tend to be healed better than the potash fractures. This is because intact potash poses much lower bulk modulus than does intact rock salt, and hence it can absorb higher strain energy. This means that under the same depth the strain energy contributes to rock salt fractures is higher than that of the potash fractures.

4) The results from the analytical solution of fracture healing after sealing in borehole indicate that the energy transfer from rock formation to the around borehole wall increases with increasing installation depth. The hydraulic aperture and intrinsic permeability decrease, and healing effectiveness increases with increasing time ( $\Delta t$ ) and applied mean strain energy ( $\Delta W_m$ ).

5) The time at which the sealing ( $t_s$ ) in underground opening is an important factor to increase the mechanical performance of the fracture healing, particularly under great depth. Under shallow depth hydraulic aperture and intrinsic permeability decrease, and healing effectiveness cannot be effectively increased because the available mean strain energy at the borehole boundary is low. The mechanical and



hydraulic performance can nevertheless be improved even under shallow depth (low mean strain energy).

6) The diagrams in Figures 6.3 to 6.5 can be used as a guideline for the seal planning and for the mechanical and hydraulic performance assessment of the fracture healing. Care should be taken carefully should to apply the results obtained here to other salt formations and locations. The mechanical properties predictions are also sensitive to the creep parameters calibrated from the laboratory test results. Application of different constitutive creep models for the surrounding salt mass may also result in different predictions of the fracture healing performance.

### **7.3 Recommendations for future studies**

Recognizing that the pressures, duration and out-flowrate used here are relatively limited. The uncertainties of the investigation and results discussed above lead to the recommendations for further studies as follows:

1. The fracture healing assessment should be performed for various durations.
2. More testing is required on a variety of specimens with different carnallite contents on fracture surface.
3. The effects of rock salt and potash inclusions on fracture surface (anhydrite, clay minerals, gypsum) should be verified for more precisely determination.
4. The effects of brine content on fractures surface should be further investigated.
5. Empirical equations in this study should be verified by field testing (in-situ stress)

## REFERENCES

- Allemandou, X. and Dusseault, M. B. (1993). Healing Processes and Transient Creep of Salt Rock. **Geotechnical Engineering of Hard Soils-Soft Rocks**. Rotterdam, Brookfield, USA: A.A. Balkema Publishers.
- ASTM D3967-95 (1998). Standard Test Method for Splitting Tensile Strength of Intact Rock Core Specimens. In: **Annual Book of ASTM Standards**. Philadelphia: American Society for Testing and Materials.
- Boussinesq, J. (1868). M Moire Sur L Influence des Frottements dans les Mouvements R guliers Des Fluids. **Journal de Mathmatiques Pure et Appliques**. 13(2): 377-424.
- Brodsky, N. S. (1990). **Crack Closure and Healing Studies in WIPP Salt Using Compressional Wave Velocity and Attenuation Measurements: Test Methods and Results**. Contract Report SAND90-7076, RE/SPEC Inc,48 p.
- Brodsky, N. S. and Munson, D. E. (1994). Thermomechanical Damage Recovery Parameter for Rock Salt From WIPP, Rock Mechanics: Models and Measurements, Challenge from Industry. In **Proceedings of the First North American Rock Mechanics Symposium** (pp. 731-738). University of Texas at Austin, Austin, Texas.
- Broek, W. M. G. T. and Heilbron, H. C. (1998). Influence of Salt Behavior on The Retrievability of Radioactive Waste. In **Proceedings of the Fourth Conference**

- on the Mechanical Behavior of Salt** (pp. 561-573). Pennsylvania State University, Montreal, Canada. Brown, E. T. and Hoek, E. (1978). Trends in Relationships Between Measured In-Situ Stresses and Depth. **International Journal of Rock Mechanics and Mining Science**. 15(4): 211-215.
- Brown, S. R. and Scholz, C. H. (1985). Broad Bandwidth Study of the Topography of Natural Rock Surfaces. **Journal of Geophysical Research: Solid Earth**. 90(B14): 12575-12582.
- Chan, K. S., Brodsky, N. S., Fossum, A. F., Bodner, S. R., and Munson, D. E. (1994). Damage-Induced Nonassociated Inelastic Flow in Rock Salt. **International Journal Plasticity**. 10(6): 623-642.
- Chan, K. S., Bodner, S. R., Fossum, A. F., and Munder, D. E. (1995). Constitutive Representation of Damage Healing in WIPP Salt. In **Proceedings of the Thirty-fifth U.S. Symposium, on Rock Mechanics** (pp. 485-490). University of Nevada, Reno, Nevada.
- Chan, K. S., Bodner, S. R., Fossum, A. F., and Munson, D. E. (1996a) Inelastic Flow Behavior of Argillaceous Salt. **International Journal Damage Mech**. 5(3): 292-314.
- Chan, K. S., Munson, D. E., Bodner, S. R., and Fossum, A. F. (1996b). Cleavage and Creep Fracture of Rock Salt. **Acta Materialia**. 44(9): 3553-3565.
- Chan, K. S., Brodsky, N. S., Fossum, A. F., Munson, D. E., and Bodner, S. R. (1997). Creep-Induced Cleavage Fracture in WIPP Salt Under Indirect Tension. **Journal of Engineering Materials and Technology**. 119(4): 393-400.

- Chan, K. S., Bodner, S. R., and Munder, D. E. (1998a). Recovery and Healing of Damage in WIPP Salt. **International Journal of Damage Mechanics**. 7(1): 143-166.
- Chan, K. S., Bodner, S. R., and Munson, D. E. (1998b). Recovery and Healing of Damage in WIPP Salt. **International Journal of Damage Mechanics**. 7(2): 143-166.
- Chan, K. S., Bodner, S. R., and Munson, D. E. (2000). Application of Isochronous Healing Curves in Predicting Damage Evolution in a Salt Structure. **International Journal of Damage Mechanics**. 9(2): 130-153.
- Chen, Z., Wang, M. L., and Lu, T. (1997). Study of Tertiary Creep of Rock Salt. **Journal of Engineering Mechanics**. 123(1): 77-82.
- Charoenpiew, P. (2015). Laboratory Study of Healing Effectiveness of Salt Fracture Under Normal Stress and Temperatures. **Master Thesis**, Suranaree University of Technology, Nakhonratchasima, Thailand.
- Colin, D. G. and Paul, R. K. (2012). **IBM SPSS statistics 19 made simple**. Psychology Press, New York.
- Costin, L. S. and Wawersik, W. R. (1980) **Creep Healing of Fractures in Rock Salt**. Report No. SAND80-0392, Sandia National Laboratories, Albuquerque.
- Fuenkajorn, K. and Phueakphum, D. (2011). Laboratory Assessment of Healing of Fracture in Salt. **Bulletin of Engineering Geology and the Environment**. 70(4): 665.
- Fuenkajorn, K. and Daemen, J. J. K. (1988). Borehole Closure in Salt. In **The Twenty-ninth US Symposium on Rock Mechanics (USRMS)**. American Rock Mechanics Association, Minneapolis, Minnesota.

- Gangi, A. F. (1978). Variation of Whole and Fractured Porous Rock Permeability with Confining Pressure. **International Journal of Rock Mechanics and Mining Sciences and Geomechanics Abstracts**. 15(5): 249-257.
- Habib, P. and Berest, P. (1993). Rock Mechanics for Underground Nuclear Waste Disposal in France: Developments and Case Studies. In **Comprehensive Rock Engineering, Geothermal Energy and Radioactive Waste Disposal**. Great Britain: Pergamon.
- Houben, M. E., ten Hove, A., Peach, C. J., and Spiers, C. J. (2013). Crack Healing in Rocksalt via Diffusion in Adsorbed Aqueous Films: Microphysical Modelling Versus Experiments. **Physics and Chemistry of the Earth**. 64: 95-104.
- Jaeger, J. C., Cook, N. G. W., and Zimmerman R. W. (2007). **Fundamentals of Rock Mechanics**. 4th ed. Australia: Blackwell.
- Katz, D. L. and Lady, E. R. A. (1976). **Compressed Air Storage**, Ann Arbor, Michigan: Ulrich's Books.
- Komenthammasopon, S. (2014). Effects of Stress Path on Rock Strength Under True Triaxial Condition. **PhD. Thesis**, Suranaree University of Technology, Nakhonratchasima, Thailand.
- Luangthip, A., Khamrat, S., and Fuenkajorn, K. (2016). Effects of Carnallite Contents on Stability and Extraction Ratio of Potash Mine. In **Proceedings of the Ninth Asian Rock Mechanics Symposium** (pp. 18-20). ISRM, Bali, Indonesia.
- Miao, S., Wang, M. L., and Schreyer, H. L. (1995). Constitutive Models for Healing of Materials with Application to Compaction of Crushed Rock Salt. **Journal of Engineering Mechanics**. 121(10): 1122-1129.

- Munson, D. E., Chan, K. S., and Fossum, A. F. (1999). **Fracture and Healing of Salt Related to Salt Caverns**. In SMRI Report, Spring Meeting paper. Solution Mining Research Institute, Las Vegas, Nevada, USA.
- Nair, K. and Boresi, A. P. (1970). Stress Analysis for Time Dependent Problems in Rock Mechanics. In **Proceedings of the second Congress of the International Society for Rock Mechanics** (pp. 1-19). ISRM, Belgrade, Serbia.
- Ouyang, S. and Daemen, J. J. K. (1989). **Crushed Salt Consolidation**. Rep. No. NUREG/CR-5402, Prepared by Department of Mining and Geological Engineering, University of Arizona.
- Peach, C. J. (1991). Influence of Deformation on the Fluid Transport Properties of Salt Rocks. **PhD. Thesis**, University of Utrecht, Holland.
- Popp, T., Minkley, W., Salzer, K., and Schulze, O. (2012). Gas Transport Properties of Rock Salt–Synoptic View. **Mechanical Behavior of Salt VII**, Leiden, Netherlands: CRC Press.
- Renard, F. (1999). **Pressure Solution and Crack Healing and Sealing**. **Institute of Geology and Department of Physics**. Charles University, Prague; Summer school on: Geology Related to Nuclear Waste Disposal, July 5-11, Roztez, Czech Republic. University of Oslo, Norway.
- Schulze, O., Popp, T., and Kern, H. (2001). Development of Damage and Permeability in Deforming Rock Salt. **Engineering Geology**. 61(2-3): 163-180.
- Snow, D. T. (1970). The Frequency and Apertures of Fractures in Rock. **International Journal of Rock Mechanics and Mining Sciences and Geomechanics Abstracts**. 7(1): 23-40.

- Stormont, J. C. (1990). Discontinuous Behavior Near Excavations in A Bedded Salt Formation. **International Journal of Mining and Geological Engineering**. 8(1): 35-36.
- Stormont, J. C. and Daemen, J. J. K. (1991). Laboratory Study of Gas Permeability Changes in Rock Salt During Deformation. **International Journal of Rock Mechanics and Mining Sciences and Geomechanics Abstracts**. 29(4): 325-342.
- Stormont, J. C. and Daemen, J. J. K. (1992). Laboratory Study of Gas Permeability Changes in Rock Salt During Deformation. **International Journal of Rock Mechanics and Mining Sciences and Geomechanics Abstracts**. 29(4): 325-342.
- Suwanich, P. (1986). Potash and Rock Salt in Thailand. **Nonmetallic Minerals Bulletin No.2. Economic Geology Division**, Department of Mineral Resources, Bangkok, Thailand.
- Tsang, Y. W. and Witherspoon, P. A. (1981). Hydromechanical Behavior of a Deformable Rock Fracture Subject to Normal Stress. **Journal of Geophysical Research: Solid Earth**. 86(B10): 9287-9298.
- Warren, J. (1999). **Evaporites: Their Evolution and Economics**. Malden, MA: Blackwell Science.
- Wilalak, N. and Fuenkajorn K. (2016). Constitutive Equation for Creep Closure of Shaft and Borehole in Potash Layers with Varying Carnallite Contents. In **Proceedings of the Ninth Asian Rock Mechanics Symposium**. ISRM, Bali, Indonesia.

Xiong, J., Huang, X., and Ma, H. (2015). Gas Leakage Mechanism in Bedded Salt Rock Storage Cavern Considering Damaged Interface. **Petroleum**. 1(4): 366-372.

Zeigler, T. W. (1976). **Determination of Rock Mass Permeability** (Technical Report S-76-2). U.S. Army Engineer Waterways Experiment Station. Vicksburg, Mississippi.





## **BIOGRAPHY**

Mister Korakot Konsaard was born on November 22, 1993 in Nakhonratchasima, Thailand. He received his Bachelor's Degree in Engineering (Geological Engineering) from Suranaree University of Technology in 2016. For his post-graduate, he continued to study with a Master's degree in the Civil, Transportation and Geo-resources Engineering Program, Institute of Engineering, Suranaree university of Technology. During graduation, 2016-2018, he was a part time worker in position of research assistant at the Geomechanics Research Unit, Institute of Engineering, Suranaree University of Technology.

